DEPARTMENT OF THE INTERIOR
U.S. GEOLOGICAL SURVEY

Geology of the Bi'r Nifazi Quadrangle, Kingdom of Saudi Arabia

by

James E. Quick 1/ and Paul S. Bosch

Open-File Report 90- 301

Report prepared by the U.S. Geological Survey in cooperation with the Deputy Ministry for Mineral Resources, Saudi Arabia

This report is preliminary and has not been reviewed for conformity with U.S. Geological Survey editorial standards and stratigraphic nomenclature.

1/ USGS, Denver, CO

1990

CONTENTS

Page

ABSTRACT....1

INTRODUCTION....2
Geographic setting....2
Previous investigations....2
Present investigation....2
Acknowledgments....4

GEOLOGIC OVERVIEW....4

PROTEROZOIC OPHIOLITIC ROCKS....4
Sedimentary, volcanic, and metamorphic rocks of the Darb Zubaydah ophiolite....6
Lower basalt....6
Basaltic breccia and tuff member....6
Kaffan sandstone....6
Lahar deposits....6
Gossan....6
Upper basalt....7
Sandstone....7
Massive tuff....7
Welded andesitic tuff....7
Welded rhyolitic tuff....7
Carbonate-replaced rock....7

INTRUSIVE ROCKS OF THE DARB ZUBAYDAH OPHIOLITE....8
Ultramafic rocks....8
Gabbro....9
Microgabbro....9
Metagabbro....9
Diabase....10
Porphyritic diabase....10
Baraq quartz diorite....10
Microcrystalline member....10
Zaynah granodiorite....11
Microcrystalline member....11
Clinopyroxene-rich member....11

POST-OPHIOLITE INTRUSIVE ROCKS....11
Umayrah complex....11
Quartz diorite....11
Quartz microdiorite....12
Granodiorite....12
Microgranodiorite....12
Magnetite vein....12
Saq'ah quartz diorite....12
Two-pyroxene gabbro....12
Nifazi granite....12

Page

Fadliyah granodiorite....12
Granite, undivided....13
Quartz monzonite....13
Sakhirah granite....13
Foliated member....13
Foliated granodiorite....13
Alkali granite....13
Alkali-feldspar granite....14
Granophyre....14
Sanam granite....14

POST-OPHIOLITE SEDIMENTARY ROCKS AND DEPOSITS....14
Jibalah group....14
Congolomerate....14
Limestone....14
Quaternary deposits....14
Terrace gravel....14
Fan deposits....15
Playa lake deposits....15
Surficial deposits, undivided....15

METAMORPHISM....15

GEOCHEMISTRY....15
Geochemical techniques....15
Results....16
Chemical suites....16
Eruptive environment....17

GEOCHRONOLOGY....26

STRUCTURE....26
Batholithic structures....26
Folding....27
Zaynah granodiorite emplacement....27
Thrust faults....27
Ghayhab fault....27
Najd faulting....28
Northeast-trending faults....28

SYNTHESIS....28

ECONOMIC GEOLOGY....29
Ore genesis....29
Nickel source....30

DATA STORAGE....30

REFERENCES....31

ILLUSTRATIONS

[Plates in pocket]

PLATES

1A. Geologic map of the Bi'r Nifazi quadrangle (northern part).
1B. Geologic map of the Bi'r Nifazi quadrangle (southern part).

FIGURES

Page

1. Index map of western Saudi Arabia showing location of the Bi'r Nifazi quadrangle.....3

2. Regional setting of the Bi'r Nifazi quadrangle.....5

3. Diagrams showing FeO vs. FeO/MgO for volcanic and hypabyssal rocks of Darb Zubaydah ophiolite.....18

4. Diagrams showing TiO_2 versus FeO/MgO for volcanic and hypabyssal rocks of Darb Zubaydah ophiolite.....19

5. Diagrams showing SiO_2 versus FeO/MgO for volcanic and hypabyssal rocks of the Darb Zubaydah ophiolite.....20

6. Diagrams showing abundances of TiO_2, Y, Nb, Ce, and Fe/Fe+Mg as a function of Zr abundance in welded tuff, granodiorite, and quartz diorite and felsite.....21

7. MgO-FeO-Al_2O_3 ternary diagrams for volcanic and hypabyssal rocks of the Darb Zubaydah ophiolite.....22

8. AFM ternary diagrams for volcanic and hypabyssal rocks of the Darb Zubaydah ophiolite.....23

9. Diagrams showing TiO_2 versus Zr for volcanic and hypabyssal rocks of the Darb Zubaydah ophiolite.....24

10. Zr-Ti-Y ternary diagrams for volcanic and hypabyssal rocks of the Darb Zubaydah ophiolite.....25

APPENDIX

Appendix A. Description of analyzed samples.....33

Appendix B. Abundances of major, minor, and trace elements, and normative minerals in representative rocks of the Bi'r Nifazi quadrangle.....35

GEOLOGY OF THE BI'R NIFAZI QUADRANGLE KINGDOM OF SAUDI ARABIA

By

James E. Quick and Paul S. Bosch

ABSTRACT

The Bi'r Nifazi quadrangle is located in the north-central part of the Precambrian shield of Saudi Arabia between lat 24° 45' and 25° 00' N. and long 41° 15' and 41° 30' E. Approximately 75 percent of the area is underlain by large plutons that range in composition from gabbro to alkali granite. A nearly complete ophiolitic section, the Darb Zubaydah ophiolite, is preserved in septa between and in roof pendants within these plutons.

The ophiolite appears to comprise the oldest rocks in the area. The age of the ophiolite (800-840 Ma) is based on a tentative correlation with dated volcanic rocks in the Nuqrah area, approximately 100 km north of the Bi'r Nifazi area.

Emplacement of younger plutons has rotated the ophiolitic section into an eastward-facing subvertical homocline. The lowest exposed unit in the ophiolite within the quadrangle is composed of serpentinized peridotite that is intruded by gabbro and diabase dikes. The serpentinite is overlain by gabbro and microgabbro, massive diabase, a lower basalt sequence, a thick sandstone sequence named the Kaffan sandstone, lahar deposits, an upper basalt sequence, and interbedded tuff, basalt, and sedimentary rocks. Tectonized peridotite is not present at the base of the ophiolite, but roof pendants of tectonized peridotite are present in the granodiorite batholith west of the Bi'r Nifazi quadrangle. The composition of volcanic rocks and the abundance of pillow basalt, volcanic wacke, and coarse-grained andesitic to rhyolitic tuff and volcaniclastic rocks suggest that the ophiolite formed in the vicinity of an island arc.

Strands of the left-lateral Najd fault system cut all of the ophiolitic and plutonic rocks and bound small basins in which sedimentary rocks of the Jibalah group were deposited.

A north-trending, 10-km-long belt of gossans crops out within the ophiolite beneath the upper-basalt sequence at Jabal Mardah. Reconnaissance drilling indicates that one of the larger gossans is underlain by a steeply

dipping, 15-m-thick, sulfide-rich volcanic wacke that averages 1 percent nickel locally. The ore is composed of pyrite, millerite, polydymite, and minor sphalerite that fill interstices between clasts of the wacke and are intimately intergrown with quartz and nickel-rich epidote and chlorite. These textures and assemblages suggest that the sulfides crystallized in situ from infiltrating hydrothermal fluids. Tuffs and basalt flows appear to have acted as impermeable barriers that channeled the hydrothermal fluids through the more permeable wacke where sulfides were deposited. Carbonate-replaced serpentinized peridotite at the base of the ophiolite is considered a potential source for the nickel. In contrast to most nickel deposits, the mineralized rocks at Jabal Mardah have extremely high Ni/Cu (130 to 260) and negligible concentrations (< 5 ppb) of platinum-group elements.

INTRODUCTION

GEOGRAPHIC SETTING

The Bi'r Nifazi quadrangle occupies an area of about 500 km^2 between lat 24°45' and 25°00' N., and long 41°15' and 41°30' E. (fig. 1). There are no paved roads within the quadrangle and the only access to the area is by desert tracks that connect with the Al Madinah-Gassim highway, located about 100 km to the northwest, or with the Mahd Adh Dhahab highway, about 150 km to the south. The topography is subdued; altitudes range from about 950 to 1,200 m, but individual hills rarely exceed 50 m from base to summit. There are no permanent settlements within the quadrangle; the only structures are a few abandoned buildings located at Bi'r Nifazi. The quadrangle is traversed by the Darb Zubaydah, an ancient caravan and pilgrimage route connecting Makkah to the south with Baghdad to the north.

PREVIOUS INVESTIGATIONS

All previous descriptions of the geology of the Bi'r Nifazi quadrangle were based on reconnaissance mapping. The Bi'r Nifazi quadrangle is located in the southeastern quadrant of the 1:500,000-scale Northeastern Hijaz quadrangle (Brown and others, 1963). Duhamel and Petot (1972) published a 1:100,000-scale map of the Al Hissu quadrangle that includes the Bi'r Nifazi that was included in the map (1:250,000) of the Al Hissu quadrangle compiled by Delfour (1981). Quick and Bosch (1989) produced a 1:50,000 reconnaissance geologic map of the eastern two thirds of the Bi'r Nifazi quadrangle as part of an investigation of the Nabitah fault zone.

Rocks of ophiolitic affinity have long been recognized in the Bi'r Nifazi area. Ultramafic and associated gabbroic rocks were mapped as part of an ophiolitic complex by Duhamel and Petot (1972) and Delfour (1981). Quick and Bosch (1989) identified a nearly complete ophiolitic section, the Darb Zubaydah ophiolite, that is floored by the ultramafic and gabbroic rocks of Duhamel and Petot (1972) and Delfour (1981), but also includes hypabyssal, volcanic, and sedimentary rocks.

The mineral potential of the Bi'r Nifazi quadrangle was considered low until reconnaissance mapping by Quick and Bosch (1989) noted that a string of large lensoidal gossans was apparently interbedded with pillow basalt and lahar deposits of the ophiolite. Preliminary geochemical results indicated that the gossans contain anomalous concentrations of nickel and cobalt. An electromagnetic survey (Bazzari, written communication, 1986) determined that electrically conducting bodies underlie the gossans, suggesting the presence of massive or interconnected sulfides at depth.

PRESENT INVESTIGATION

The Bi'r Nifazi quadrangle was selected for detailed mapping because of the economic potential represented by outcrops of gossan. Attention was

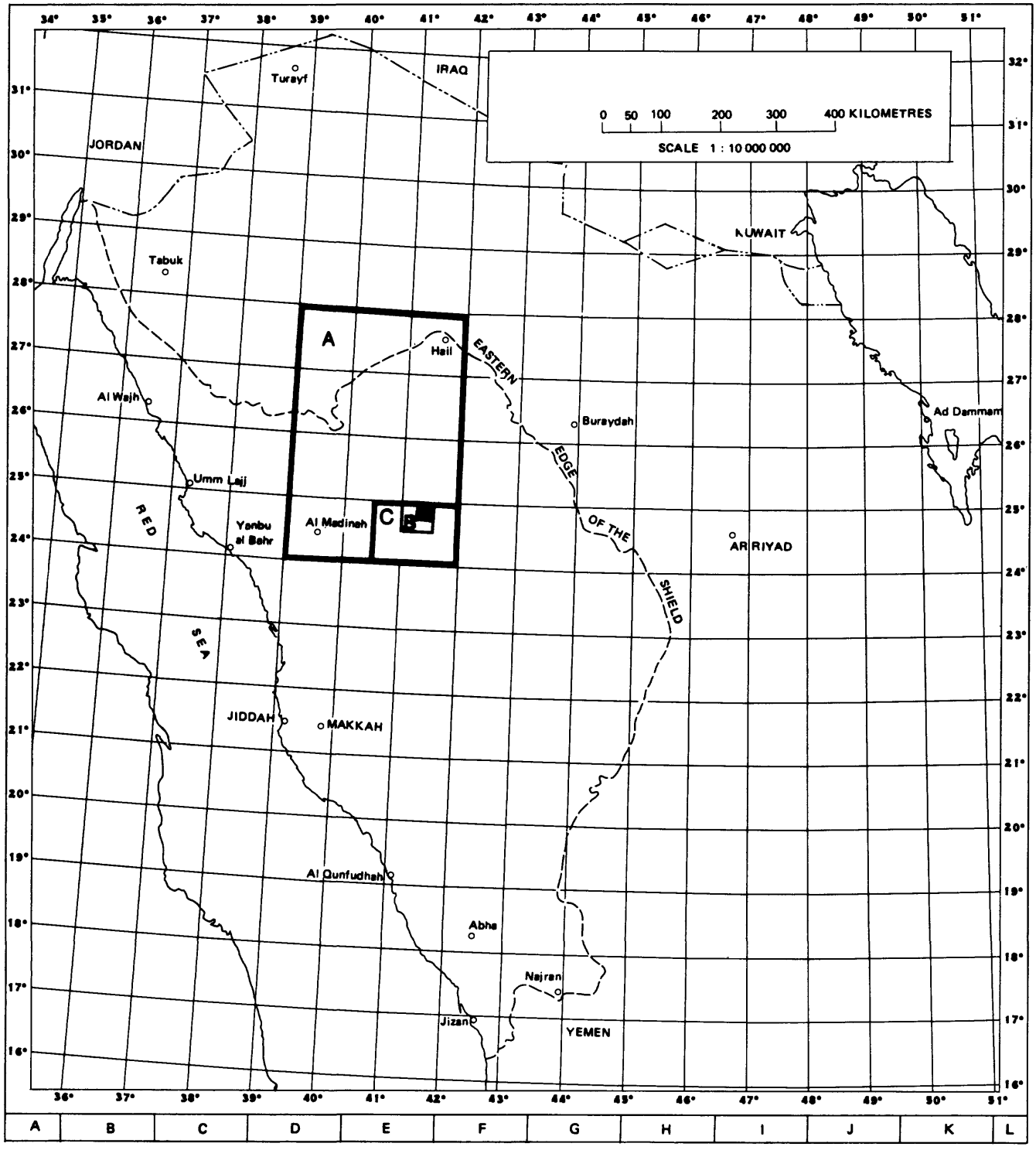

Figure 1.– Index map of western Saudi Arabia showing location of the Bi'r Nifazi quadrangle (shaded) and areas mapped by Brown and others (1963), A; Duhamel and Petot (1972), B; and Delfour (1977, 1981), C.

focused on the Darb Zubaydah ophiolite to establish the geologic environment of the mineralization. This project was conducted concurrently with a prospect evaluation of the individual gossans (Bosch and others, in preparation).

The Darb Zubaydah ophiolite, which underlies about 25 percent of the total area, was mapped at a scale of 1:10,000. Granitic rocks that underlie the remainder of the quadrangle were mapped at a scale of 1:25,000. The geology was compiled at a scale of 1:25,000 (plate 1). The concentrations of selected major and trace elements were measured in 145 samples.

ACKNOWLEDGMENTS

Aerial photographs were prepared for this investigation by the U.S. Geological Survey photography laboratory under the direction of Khaled Hajiraf. Steve Jarvis (Saudia Special Flights) flew numerous graphic missions. Mir Amjod Hussein and Abdul Malek Helaby performed the major- and trace-element analyses, respectively. Helpful technical reviews of the manuscript were provided by E. duBray and J. Cole.

GEOLOGIC OVERVIEW

The Bi'r Nifazi quadrangle is located in the Nuqrah belt, an extensive terrane of volcanic and sedimentary rocks (fig. 2). These rocks are significant both for the information they convey about the earliest geologic and tectonic environment of the north-central Arabian shield and for their economic potential. Rocks of the Nuqrah belt were formed in an island-arc environment (Delfour, 1977; Johnson, 1983) about 800-830 million years ago (Calvez and others, 1983). The Nuqrah belt was later intruded by enormous volumes of granitic rocks that range in composition from quartz diorite to alkali-feldspar granite. The Nuqrah belt is known to host massive-sulfide and vein-gold deposits (Smith and Johnson, 1986).

Within the Bi'r Nifazi quadrangle, volcanic and sedimentary rocks of the Nuqrah belt comprise the top of an ophiolitic section named the Darb Zubaydah ophiolite (Quick and Bosch, 1989). Within the quadrangle, the ophiolite is exposed in a pair of north-trending, nearly contiguous septa that are truncated in the south by a major left-lateral strike-slip fault. Volcanic rocks of the ophiolite range in composition from tholeiitic basalt to low-potassium rhyolite. Associated gabbro, microgabbro, diabase, quartz diorite, and granodiorite are interpreted to be the plutonic and hypabyssal equivalents of these rocks. The compositions of the volcanic rocks and the presence of interbedded wacke, shale, and lahar deposits suggest an island-arc origin for the ophiolite.

Approximately three quarters of the quadrangle is underlain by post-ophiolite plutonic rocks that range in composition from alkali-feldspar granite to gabbro. The ophiolite is split into two septa by quartz-diorite and granodiorite of the Umayrah complex. To the east, the ophiolite is flanked by the Nifazi granite and the Saq'ah quartz diorite, and to the west by the Fadliyah granodiorite. The ophiolite is also cut by numerous small intrusions composed of two-pyroxene gabbro, quartz diorite, granodiorite, and granite.

PROTEROZOIC OPHIOLITIC ROCKS

The Darb Zubaydah ophiolite crops out in a steeply dipping homocline that contains, from west to east (1) undivided ultramafic and mafic rocks, (2) gabbro, (3) diabase, (4) quartz diorite and granodiorite; (5) basalt flows and tuff, (6) volcanogenic sandstone and lahar deposits, (7) pillow basalt and gossan; and (8) interbedded sedimentary and intermediate- to rhyolitic-composition volcanic rocks. These rocks, considered collectively, approximate the sequence of lithologies that define an ophiolite (Anonymous, 1972).

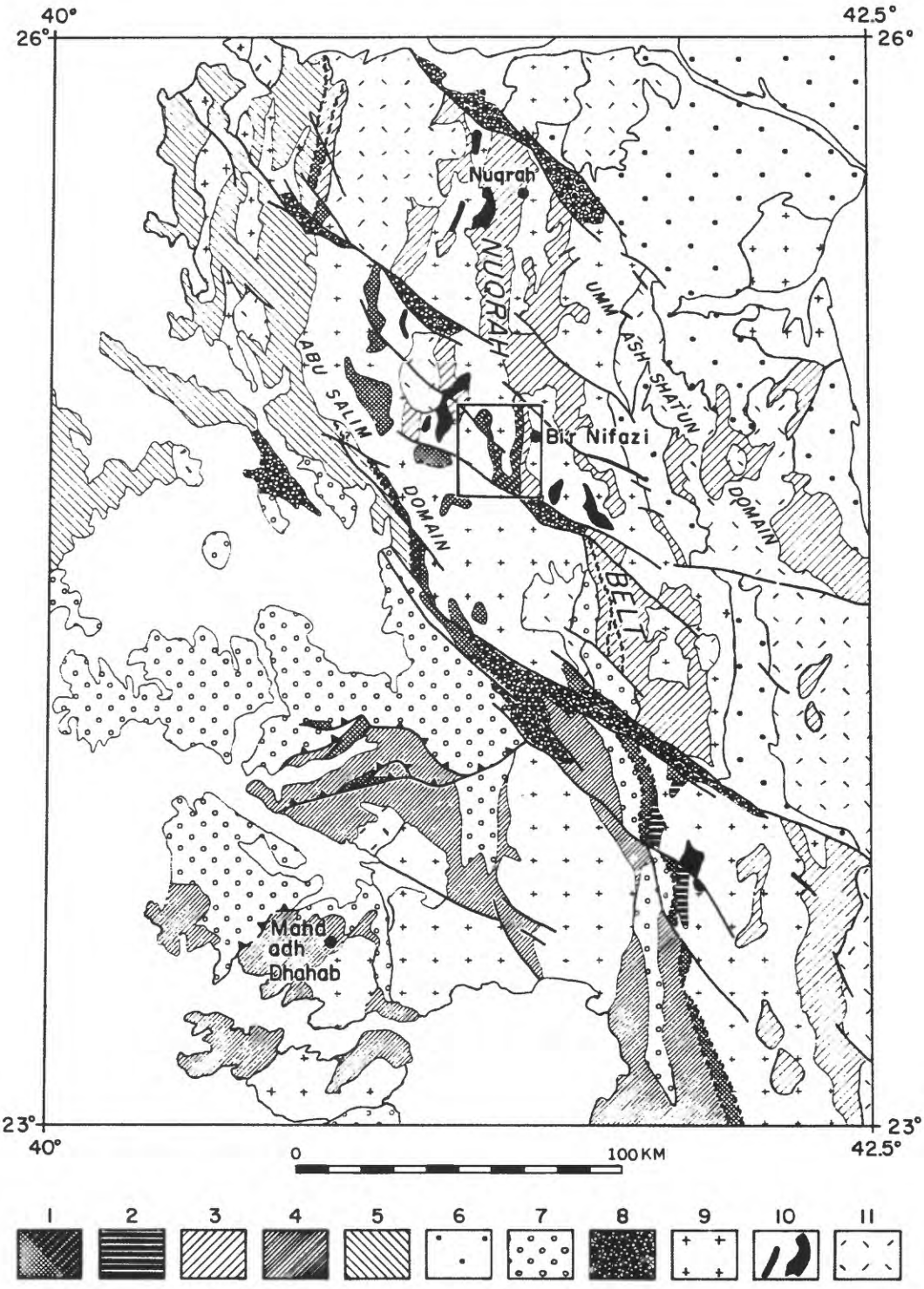

Figure 2.-- Regional setting of the Bi'r Nifazi quadrangle: (1) ophiolitic serpentinite (grid) and gabbro/diabase (grid+inclined bars), (2) amphibolite, (3) volcanic & sedimentary rocks of Nuqrah belt, (4) volcanic & sedimentary rocks older than 800 Ma, (5) volcanic & sedimentary rocks younger than 800 Ma, (6) Murdama group, (7) sedimentary & volcanic rocks of the Furayh group, (8) sedimentary & volcanic rocks of the Jibalah group, (9) granodiorite, tonalite, and diorite, (10) Rharaba complex, and (11) undivided granitic rocks. Faults: broken wavy lines, Nabitah faults; heavy lines, Najd faults; and barbed lines, north-dipping thrust faults of Bi'r Umq suture.

SEDIMENTARY, VOLCANIC, AND METAMORPHIC ROCKS OF THE DARB ZUBAYDAH OPHIOLITE

Lower Basalt (bl)

Interbedded basaltic flows and tuff that crop out near Wadi Ghayhab in the southeastern corner of the quadrangle are mapped as the lower basalt of the Darb Zubaydah ophiolite. Dark- to medium-gray-green basaltic flows and flow breccia are interbedded with basaltic tuff, volcanic wacke, and minor keratophyre; vesicles are locally abundant. Pillow structures are locally well perserved, although, in general, they are difficult to recognize due to pervasive fracturing of the rocks. Interbedded andesite and andesitic breccia contain abundant fragments of volcanic rock.

The primary mineralogy of the rocks consists of subophitic to eutaxitic intergrowths of plagioclase, clinopyroxene(?), and opaque minerals. Plagioclase is intensely saussuritized, and primary mafic silicates are completely replaced by chlorite and epidote. The groundmass is replaced by an extremely fine-grained intergrowth of albite, chlorite, epidote, and opaque minerals.

Basaltic Breccia and Tuff Member (bb): Within the lower basalt sequence, interbedded basaltic flow breccia and tuff are mapped as a separate unit where they are thick enough to depict at map scale. Flow breccias are clast-supported aggregates of angular blocks of basalt 1 to 50 cm in diameter. The interstices between blocks are filled with calcite. In many places, flow breccia grades upward into tuff with decreasing clast size. Crossbedding in the basaltic tuff indicates that stratigraphic up is toward the east.

Kaffan Sandstone (sk)

The lower basalt is overlain by a thick unit of interbedded volcanic wacke and lesser amounts of mudstone, shale, lahar deposits, and minor ferruginous marble. Because of their stratigraphic significance and extent of exposure, these rocks have been assigned to the Kaffan sandstone, an informal formation name. The word "kaffan" (Arabic for shroud) is without geographic significance: it refers to the manner in which this unit completely covers the lower basalt.

The Kaffan sandstone ranges from siltstone to coarse-grained conglomeratic sandstone and is composed of poorly sorted angular fragments of volcanic rock and feldspar. The volcanic rock fragments are predominantly plagioclase-phyric andesite. Bedding thickness ranges from laminated (for shale, siltstone, and fine-grained sandstone) to massive (for mudstone and coarse-grained sandstone. Incomplete Bouma cycles are abundant suggesting that the sandstones are turbidites. Graded bedding and crossbedding indicate that stratigraphic up is toward the east.

The Kaffan sandstone has been disrupted by emplacement of hypabyssal sills and by extensive bedding-plane faulting. Nevertheless, it forms a coherent unit that can be traced from the southern quadrant of the quadrangle, where it is 300-500 m thick, to the northern edge of the quadrangle, where it is at least 1000 m thick. Northward thickening of the Kaffan sandstone and the predominance of andesitic to Na-rhyolitic volcanic clasts suggest that the Kaffan sandstone was deposited by turbidity currents that deposited sediments from a calc-alkaline volcanic center in the south to a major depositional basin in the north.

Lahar Deposits (l): Boulder-rich mudstones and sandstones that crop out near the top of Kaffan sandstone are mapped as lahar deposits of the Kaffan stone. These rocks are composed of angular to rounded clasts that are completely suspended in a carbonate-rich matrix that grades from mudstone to fine-grained, poorly sorted sandstone. The clasts are composed of basalt, andesite, dacite, Na-rhyolite, limestone, and minor diorite. Ellipsoidal clasts are generally oriented with long axes parallel to the bedding plane.

Lahar deposits appear to increase gradually in thickness from south to north, although this could be an artifact of bedding-plane faulting. At Jabal Mardah, lahar deposits terminate abruptly along strike against basalt in a relationship interpreted to be a buttress unconformity where lahar deposits accumulated against an active fault scarp.

Gossan (g)

Gossan crops out near the contact of the upper basalt and the lahar deposits. Outcrops composed of rusty-red weathering siliceous ironstone range from a few meters to as much as 80 m wide and 400 m long. The extent of apparent stratigraphic

control on the gossans is remarkable. A chain of gossans extends southward from the Jabal Mardah area for 10 km. A second chain extends northward from the southern boundary of the quadrangle for 8 km. In both chains, the gossans occur near the base of the upper basalt.

Upper Basalt (b)

Lahar deposits are overlain conformably by pillow basalt interbedded with minor wacke, marble, and chert. The pillow basalt is medium gray to gray green, pervasively fractured, and locally vesicular. The rounded shapes seen in outcrops are interpreted to be pillow structures on the basis of isolated examples of well-preserved pillows. Relict textures indicate that the basalt was originally composed of subophitic intergrowths of plagioclase, pyroxene, olivine(?), and opaque minerals. However, the primary minerals were extensively replaced during greenschist-facies alteration. The plagioclase is highly saussuritized and the pyroxene is completely uralitized. Olivine is inferred to have been a primary mineral of the basalt on the basis of small patches of serpentine. Calcite and epidote form veinlets, fill vesicles, and replace patches of groundmass within the basalt. The abundance of calcite and epidote increases dramatically near the Wadi Ghayhab faults.

Sandstone (s)

Lenses of sandstone interbedded with siltstone, shale, and chert are contained within the upper basalt sequence and the massive tuff. These lenses are mapped as sandstone where their thickness is significant.

Massive Tuff (t)

The upper basalt sequence is conformably overlain by massive tuff interbedded with minor sandstone, welded andesitic tuff, and basalt. The contact with the underlying basalt is gradational with basalt becoming less abundant up section relative to the tuff. The tuff is dark-gray and massive, and ranges in composition from basalt to andesite (see CHEMISTRY). In most places, it is composed of an intergrowth of tiny (0.3-1 mm), saussuritized plagioclase phenocrysts contained in an extremely fine-grained (<0.03 mm), mosaic-textured matrix of feldspar, quartz, opaque minerals, chlorite, epidote, and scarce biotite. Microphenocrysts are locally skeletal; in some rocks, they display a planar preferred orientation.

There is considerable lithologic variation from north to south in the tuff unit. In the south, angular clasts are abundant. To the north, clasts decrease in size and become less abundant, and much of the tuff appears to have been reworked. These characteristics suggest that the source area(s) and volcanic center(s) were located to the south.

Welded Andesitic Tuff (dc)

Welded andesitic tuff is interbedded with the massive tuff north of Wadi Ghayhab. Individual units are about 50 to 100 m thick. The welded andesitic tuff is light to medium gray, fissile, and contains abundant flattened pumice clasts. It is composed of tiny (< 1 mm) resorbed quartz phenocrysts set in a mosaic-textured felsite ground-mass of minute (<0.02 mm) grain size.

Welded Rhyolitic Tuff (wt)

Welded rhyolitic tuff crops out in the southeast corner of the quadrangle where it is interbedded with the massive-tuff unit. The welded rhyolitic tuff is composed of numerous, thick welded ash flows. These rocks weather dark gray to to orange, contain abundant flattened pumice clasts (interpreted to be fiamme), are fissile, and are composed of quartz phenocrysts (<0.5 mm) and moderately saussuritized oligoclase set in a very fine-grained (< 0.03 mm) mosaic-textured felsite. The pumice clasts are extensively replaced by chlorite and epidote. Fractures and vugs are filled by calcite, epidote, and chlorite. Welding suggests subareal deposition; drag folds present in individual units suggest that paleotopography sloped downward to the north.

Carbonate-Replaced Rock (cr)

Carbonate-replaced rock underlies large areas near Jabal Mardah and smaller areas within fault zones and in roof pendants in quartz diorite near Wadi Umayrah (near sample site 362). Near Jabal Mardah, pillow basalt and Kaffan sandstone(?) have been almost completely replaced by a buff-weathering assemblage of carbonate minerals. The basaltic heritage of some of these rocks is indicated by preservation of small (<10 cm) relics of gray-green basalt.

INTRUSIVE ROCKS OF THE DARB ZUBAYDAH OPHIOLITE

ULTRAMAFIC ROCKS (um)

Ultramafic rocks intruded by dikes, sills, and small plugs of gabbro and diabase crop out along the western limit of the Darb Zubaydah ophiolite. These rocks represent the deepest structural level of the ophiolite that is exposed within the quadrangle.

The ultramafic rocks are composed of intensely serpentinized peridotite that is recessive weathering relative to the diabase and gabbro. Outcrops are buff, white, and various shades of green. Veins of cross-fiber chrysotile almost 1 cm wide are abundant. Precise identification of the protolith is prevented by the intensity of the alteration. Nevertheless, pyroxene-bearing peridotite and dunite are distinguished by the presence or absence of bastite and carbonate pseudomorphs after pyroxene, respectively; on this basis, dunite is estimated to make up 60-80 percent of the ultramafic rocks. In contrast, dunite rarely exceeds pyroxene-bearing peridotite in abundance within the ultramafic tectonites of most ophiolites (Coleman, 1977).

Spinel foliation, which is commonplace in most ophiolites and is considered to be evidence of deformation under mantle conditions (e.g., Boudier, 1978), is scarce in the ultramafic rocks of the Darb Zubaydah ophiolite. However, a west-dipping foliation (located about 3 km south of Jabal Sakhirah) defined by flattened spinel grains is locally pronounced.

The extreme alteration of the primary mineralogy is remarkable even for ultramafic rocks. Primary silicate minerals have been completely replaced by serpentine, talc, chlorite, dolomite, and magnetite. X-ray defraction analysis indicates that lizardite is the dominant serpentine polymorph in the Bi'r Nifazi area. Primary chromium-spinel has formed extensive pseudomorphs after magnetite, and primary chromium-spinel is only preserved in the cores of magnetite-rimmed grains.

The Cr/Cr+Al ratios in chromium-spinel range from 0.75 to 0.85. This range is higher and more restricted than that found in spinels in peridotite dredged from midocean ridges and fracture zones, and is more typical of spinels in island-arc volcanic rocks and ultramafic cumulates (Dick and Bullen, 1984).

The ultramafic rocks of the Darb Zubaydah ophiolite are interpreted to have formed as cumulates in a crustal environment, based on (1) the scarcity of a penetrative spinel foliation characteristic of mantle tectonites, (2) the high Cr/Cr+Al values of the spinels, (3) local bastite psuedomorphs after pyroxene that preserve a poikilitic texture, and (4) the abundance of dunite. In contrast, ultramafic rocks displaying penetrative spinel foliation crop out in roof pendants within granodiorite located 10-15 km west and southwest of the Bi'r Nifazi quadrangle. Significantly, spinels from these rocks have lower chromium contents (Cr/Cr+Al = 0.47-0.81) that are more similar to chromium contents of spinels in ultramafic tectonites of ophiolites. This spatial relationship suggests that the boundary between crustal and mantle parts of the ophiolite, or the "petrologic Moho", is west and southwest of the ultramafic rocks in the Bi'r Nifazi quadrangle, but has been obscured by granodiorite intrusions.

Gabbro and diabase form north-striking layers within the ultramafic rocks that constitute 30-50 percent of the exposed rock and form black ridges that project 2-3 m above the ultramafic host rock. These layers dip vertically to 45° to the west and are fragmented into boudins, and enveloped by rodingite, blackwall, and talc-actinolite reaction zones. Such reaction zones develop between mafic and ultramafic rocks during serpentinization and demonstrate that the gabbro and diabase were in contact with the ultramafic rocks prior to serpentinization.

Subophitic textures are preserved in the interiors of the gabbro and diabase layers. Grain sizes range from about 0.5 mm to 2 mm but, in general, grain size is relatively uniform within a single layer. Layers are devoid of cumulus textures.

The relationship between these mafic and ultramafic rocks is obscured by alteration and deformation. Due to the fine-grain size and the absence of cumulus features, the mafic layers are thought to have intruded the ultramafic rocks rather than crystallized as cumulus layers.

GABBRO (gb)

Fine- to medium-grained gabbro underlies dark-brown to black, rugged, boulder-covered hills directly east of the undivided ultramafic and mafic rocks.

The primary minerals of the gabbro have been extensively altered, although the primary cumulus texture is preserved. Pyroxene is completely replaced by green amphibole, plagioclase is replaced by a very fine-grained mosaic of albite, quartz, and zoisite, and the only surviving primary minerals are equant, euhedral magnetite grains. The rocks are cut by quartz- and epidote-filled veins.

The internal structure of the gabbro is not well known and identification of intrusive units and structures is difficult. Outcrops tend to be small and isolated by talus-covered slopes. In general, however, the rocks appear to be massive and devoid of cumulus layering. Abrupt changes in grain size and mineralogy are commonplace. This observation, coupled with the paucity of coarse-grained gabbro and cumulus structures, suggests that the gabbro is composed of numerous small intrusions rather than a single body crystallized in a large magma chamber.

The diabase and gabbro layers in the ultramafic rocks may have been feeders for the overlying gabbro. There are no discernable petrographic differences between the massive gabbro and the gabbro layers in the ultramafic rocks. The eastern contact of the ultramafic rocks is marked by an interleaving of ultramafic and gabbroic rock and a gradual increase to the west in the ratio of serpentinite to gabbro. The absence of cumulus structures at the contact suggests that the gradation does not reflect the magmatic evolution of a single differentiating pluton. The presence of boudinage and shearing along gabbro-serpentinite contacts indicates that the transition from serpentinite to gabbro has been complicated by deformation. Nevertheless, the gradation from serpentinite to gabbro is reminiscent of the Preston ophiolite, where diabase and gabbro dikes intrude ultramafic rocks and coalesce upward into massive diabase and fine-grained gabbro that lacks cumulus layering (Snoke and others, 1981).

MICROGABBRO (dg)

Extremely fine-grained mafic intrusive rocks are collectively mapped as microgabbro in the south-central part of the Bi'r Nifazi quadrangle. The rocks are massive and weather dark-brown to black. They are extremely resistant and underlie the most rugged terrane in the Darb Zubaydah ophiolite.

Primary minerals, such as those in the underlying gabbro, are profoundly altered. Pyroxene is completely replaced by blue-green amphibole and plagioclase is completely recrystallized to a very fine-grained mosaic of quartz, feldspar, and zoisite. Quartz- and epidote-filled veins are abundant.

The contact with the gabbro to the west is not exposed. Although the microgabbro unit is typically much finer grained than the gabbro, the microgabbro includes rocks that are properly termed fine-grained gabbro. Some of these gabbro bodies form mappable dikes that cut the diabase. This suggests that the transition from gabbro to diabase may be gradational and reflects intrusion into higher and, therefore, cooler levels in the crust where microgabbro would crystallize in small intrusions and gabbro would crystallize only in larger intrusions.

A classic ophiolitic sill-and-dike complex (Coleman, 1977) was not observed in the Bi'r Nifazi quadrangle. Individual intrusions are large and shapes are difficult to delineate because of the intense fracturing of the rocks and their poor exposure. As in the gabbro, intrusive contacts may be defined in some outcrops on the basis of abrupt changes in grain size or mineralogy. The attitudes of these contacts tend to dip steeply and strike north to northeast. A similar attitude is displayed by mapped gabbro dikes.

Locally, the diabase is intensely fractured, and quartz-epidote veins fill cracks between angular blocks. In some outcrops, the rocks superficially resemble a volcanic breccia. However, blocks tend to be irregular and angular in shape, and shapes tend to match across the quartz-epidote veins, suggesting that the rocks were "healed" in situ after fracturing. Fracturing may have occured in response to faulting, emplacement of another diabase intrusion, or a process analogous to hydraulic fracturing.

METAGABBRO (md)

Metadiabase and metagabbro crop out in the northern third of the quadrangle near Wadi al Umayrah. The rocks are fine- to medium-grained,

foliated amphibolite composed of a mosaic-textured intergrowth of greenish-brown hornblende, calcic andesine and opaque minerals. They are interpreted to be the metamorphosed equivalent of the gabbro and microgabbro based on their composition (basic) and location on strike with those units.

DIABASE (d)

Diabase crops out as a large sill-like body near Wadi Ghayhab (in the southern half of the quadrangle) and forms smaller sills and dikes in the overlying volcanic rocks. In contrast to the microgabbro, these rocks display a clear diabasic texture in hand specimen and underlie low, gently rounded hills.

The primary mineralogy of the diabase was a subophitic intergrowth of small (< 1mm) plagioclase laths, interstitial clinopyroxene, and opaque minerals. Clinopyroxene is almost completely altered to green hornblende and chlorite, and plagioclase is highly saussuritized.

The fine grain size of the diabase suggests that it is composed of multiple, small intrusions, rather than a single large body. Although individual intrusive units within the diabase are obscured by intense fracturing and poor exposure, attitudes of contacts between intrusive bodies suggest that the unit is composed of a series of north-trending, steeply dipping dikes and sills.

The diabase is inferred to be part of the ophiolite on the basis of its chemical similarity to rocks of the upper basalt sequence (see CHEMISTRY). However, the diabase unit appears to have been emplaced relatively late in the evolution of the ophiolite. The diabase contains xenoliths and screens composed of rocks of the lower basalt and the Kaffan sandstone. The large, sill-like diabase body intrudes the lower basalt sequence, the Kaffan sandstone, and the overlying lahar deposits. Smaller diabase bodies intrude the upper basalt and massive tuff.

PORPHYRITIC DIABASE (dp)

Porphyritic diabase crops out between Wadi al Umayrah and Wadi Ghayhab. This unit is distinguished from the diabase by abundant small (<2 mm) plagioclase phenocrysts. It weathers medium-gray and, like the diabase, is highly fractured and underlies low, rounded hills.

In the northern part of the quadrangle, the porphyritic diabase forms sills that intrude the lower basalt and the Kaffan sandstone, and contains screens and xenoliths of volcanic and sedimentary rocks. Local dike-on-dike intrusions of porphyritic diabase are present. In many places, the porphyritic diabase appear to be an intrusive breccia, containing angular fragments of porphyritic diabase that are distinguished from the host intrusion by their slightly darker color. These internal structures and the uniform fine grain size of the porphyritic diabase suggest that it was formed from numerous small intrusions.

BARAQ QUARTZ DIORITE (qdb)

A 5-km-long, recessive-weathering pluton of hornblende quartz diorite is designated as the Baraq quartz diorite, after outcrops on the east flank of Jabal Al Baraq. The rocks range from medium grained in the south to extremely fine grained to aphanitic in the north. The medium-grained (1-2 mm) rocks are composed of euhedral plagioclase enclosed in poikilitic hornblende; interstices are filled by quartz and minor opaque minerals. With decreasing grain size, the rock grades into an extremely fine-grained (< 0.3 mm) hypidiomorphic intergrowth of amphibole, quartz, plagioclase, and opaque minerals. Locally, the Baraq quartz diorite contains mosaic-textured, biotite-rich xenoliths. Extremely fine-grained dikes of Baraq quartz diorite intrude the diabase porphyry to the west.

Microcrystalline Member (f)

Buff- to light-green-colored microcrystalline quartz diorite forms an 8-km-long sill-like body that extends northward from Jabal Al Baraq along the eastern margin of the diabase unit. The microcrystalline quartz diorite and the Baraq quartz diorite are interpreted to constitute a single elongate intrusion that has been disrupted by faulting. The felsite is composed of tiny (< 1 mm) phenocrysts of hornblende, plagioclase, and quartz contained in an extremely fine-grained (< 0.03 mm), felty, opaque-rich groundmass. Dikes of the microcrystalline quartz diorite intrude the diabase unit. Although the microcrystalline quartz diorite is not in contact with the Baraq quartz diorite, the two units are similar in composition (see CHEMISTRY). The Baraq quartz

diorite grades into a rock very similar in appearance to the microcrystalline quartz diorite with decreasing grain size to the north.

ZAYNAH GRANODIORITE (gdz)

The Zaynah granodiorite is a small pluton of hornblende granodiorite that crops out at Jabal Zaynah near the southern margin of the quadrangle. The rock is recessively weathering, white, and medium grained to extremely fine grained. It is composed of a hypidiomorphic-granular intergrowth of subhedral hornblende and plagioclase; interstices are filled by quartz and minor alkali feldspar. Alteration has saussuritized plagioclase and introduced secondary muscovite, chlorite, and calcite. Large sills of Zaynah granodiorite intrude contacts between the diabase, the lower basalt, and the Kaffan sandstone.

Microcrystalline Member (c)

Extremely fine-grained granodiorite is mapped as the microcrystalline member of the Zaynah granodiorite. The microcrystalline member crops out on the eastern side of Wadi Ghayhab, where it forms a chilled margin on coarser-grained Zaynah granodiorite, and on the western side of Wadi Ghayhab, where it forms a small satellite sill in the lower basalt and Kaffan sandstone.

The microcrystalline member is composed of small (< 1 mm), zoned plagioclase and rounded quartz phenocrysts contained in an extremely fine-grained (< 0.03 mm) felsic groundmass. Secondary chlorite and muscovite are abundant. Dikes of microcrystalline granodiorite as much as 1 m thick (not shown on Plate 1) intrude the Zaynah granodiorite, the Kaffan sandstone, and the upper basalt, but are absent from the country rocks on the east side of the Zaynah granodiorite. This observation suggests that the Zaynah granodiorite was intruded into the ophiolite as a sill that radiated dikes upward into the overlying Kaffan sandstone and volcanic rocks, and that subsequent regional deformation rotated the sandstone, basalt, and granodiorite approximately 90 degrees into their present orientation.

Clinopyroxene-Rich Member (mgdz)

Clinopyroxene-rich gabbro forms small sills in the Kaffan sandstone and overlying volcanic rocks east and northeast of Jabal Zaynah. Plagioclase fills interstices between euhedral, green clinopyroxene. The amount of plagioclase is variable and, locally, the rock grades into clinopyroxenite. The occurence of the clinopyroxene-rich gabbro is restricted to the vicinity of the Zaynah granodiorite, which suggests that the two rock types may be consanguineous.

POST-OPHIOLITE INTRUSIVE ROCKS

UMAYRAH COMPLEX

The Umayrah complex is a large composite diorite to granodiorite plutonic mass that is centered on Wadi Umayrah. Apophyses of the Umayrah complex intrude the gabbro, microgabbro, diabase, and porphyritic diabase of the Darb Zubaydah ophiolite and roof pendants of metadiabase, metagabbro and Kaffan sandstone are contained within the complex. The complex is divided into quartz diorite, microquartz diorite, granodiorite, and microgranodiorite. The microcrystalline units are symmetrically distributed on both east and west flanks of the complex, suggesting that they are chilled margins on a large pluton emplaced essentially in its present orientation. Therefore, the Umayrah complex is inferred to have intruded the Darb Zubaydah ophiolite after it was rotated into a nearly vertical orientation.

Quartz Diorite (qd)

Quartz diorite of the Umayrah complex underlies broad areas on both banks of Wadi Umayrah north of Jabal Aftah. The quartz diorite weathers to pediments and low hills that are covered in many places by a thin layer of gruss produced by its disintegration. It is white to light gray in color (color index < 20) and is composed of a medium-grained (0.5-2 mm) hypidiomorphic-granular intergrowth of hornblende, plagioclase, quartz, minor opaque minerals, and trace amounts of alkali feldspar.

Quartz Microdiorite (mqd)--Quartz diorite grades into quartz microdiorite as grain size deceases near contacts with the country rock. The quartz microdiorite is medium gray to buff color and underlies low rounded hills that rise above the quartz diorite. It is composed of (< 2 mm) plagioclase and hornblende phenocrysts set in a fine-grained (<0.03 mm), mosaic-textured felsic matrix. Hornblende is almost completely altered to chlorite, and plagioclase is highly saussuritized.

Granodiorite (gd)

Medium-grained hornblende granodiorite crops out on the east flank of Jabal al Ghirah. Like the quartz diorite, it is recessive weathering and white to light-gray in color. The granodiorite is composed of a hypidiomorphic-granular intergrowth of quartz, plagioclase, potassium feldspar, and minor amounts of hornblende and opaque minerals. It is distinguished from the quartz diorite by visible alkali feldspar in hand specimen.

Microgranodiorite (mgd)--Granodiorite grades into microgranodiorite with decreasing grain size near contacts with the country rocks. Microgranodiorite crops out extensively at Jabal al Baraq and Jabal al Ghirah. The rock is identical in appearance to the quartz microdiorite, its color ranging from medium-gray to buff color and underlying low, rounded hills. It is composed of small (0.5-3 mm), plagioclase phenocrysts set in an extremely fine-grained (<0.03 mm) groundmass of mosaic-textured, chlorite-rich felsite. However, compared to the microquartz diorite, the microgranodiorite is characterized by a higher potassium content (Table 1) and is, therefore, mapped separately as an aphanitic phase of the granodiorite.

Magnetite Vein

A 3-m-wide, 30-m-long vein of massive magnetite cuts quartz diorite of the Umayrah complex near the northern edge of the quadrangle in Wadi al Umayrah. The age of the mineralization is unknown.

SAQ'AH QUARTZ DIORITE (qds)

A large pluton of hornblende quartz diorite underlying Jabal Saq'ah is mapped as the Saq'ah quartz diorite in the northeast part of the quadrangle. The Saq'ah quartz diorite is distinguished from the dioritic rocks of the Umayrah complex by a uniformly fine grain size and higher color index (20-30). It is also more resistant to weathering and forms low hills. The Saq'ah quartz diorite is clearly younger than the Darb Zubaydah ophiolite; west of Bi'r Nifazi, a large dike of Saq'ah quartz diorite intrudes massive tuff of the ophiolite.

The age of the Saq'ah quartz diorite relative to the Umayrah complex is unknown.

TWO-PYROXENE GABBRO (gb2)

Dikes and plugs of two-pyroxene gabbro intrude the serpentinite and volcanic rocks of the Darb Zubaydah ophiolite, and the younger Umayrah complex. It weathers to large, distinctive blue-green boulders. These gabbro bodies are distinguished from the ophiolitic gabbro by the presence of two pyroxenes, coarser grain size, and a significantly lower degree of alteration.

NIFAZI GRANITE (gn)

The southeastern margin of the quadrangle is underlain by a large alkali-feldspar-rich granite pluton that is defined as the Nifazi granite from exposures at Bi'r Nifazi. The granite is recessive weathering, colored red, and ranges in composition from syenogranite to alkali-feldspar granite. It is composed of a medium-grained (0.3-3 mm) hypidiomorphic intergrowth of microcline, quartz, and minor amounts of plagioclase, biotite, opaque minerals, and, locally, aegirine. Roof pendants of recrystallized, ophiolitic volcanic rocks are abundant within the Nifazi granite, and dikes and apophyses of Nifazi granite extensively intrude the Darb Zubaydah ophiolite, the two-pyroxene gabbro, and the Saq'ah quartz diorite. The age of the Nifazi granite relative to the Umayrah complex is unknown.

FADLIYAH GRANODIORITE (gf)

The northwestern quarter of the quadrangle is underlain by a vast granodiorite body that is named the Fadliyah granodiorite after exposures at Jabal Fadliyah. The Fadliyah granodiorite is bounded to the south by a major left-lateral, strike-slip fault of the Najd fault system. The Fadliyah granodiorite is part of a vast exposure of granitic rocks referred to as the Abu Salim granite domain (Delfour, 1981).

The Fadliyah granodiorite is composed of mostly medium- to coarse-grained hornblende granodiorite. These rocks are light gray to white, recessive weathering, and typically underlie gruss-covered plains. They are composed of a hypidiomorphic-granular intergrowth of subhedral hornblende and plagioclase, and euhedral potassium feldspar; interstices are filled by quartz and potassium feldspar. Hornblende is partially replaced by chlorite and plagioclase is moderately saussuritized.

The granodiorite is extensively intruded by abundant dikes and small irregular bodies of alkali-feldspar granite, which are more resistant and form low hills and ridges.

The Fadliyah granodiorite intrudes the ultramafic rocks of the Darb Zubaydah ophiolite; it contains roof pendants of tectonized peridotite about 10-15 km west of the Bi'r Nifazi quadrangle. North of Wadi Umayrah, an apophysis of the Fadliyah granodiorite intrudes quartz diorite of the Umayrah complex. Fadliyah granodiorite also intrudes the two-pyroxene gabbro northwest of Jabal Aftah and contains pendants of two-pyroxene gabbro north of Wadi Umayrah. The age of the Fadliyah granodiorite relative to the Saq'ah quartz diorite and Nifazi granite is unknown.

GRANITE, UNDIVIDED (gu)

Much of the southwestern quadrant of the quadrangle is underlain by rocks that range in composition from quartz monzonite to alkali-feldspar granite that is separated from the Fadliyah granodiorite by a major left-lateral, strike-slip fault. Although similar in outcrop appearance to the Fadliyah granodiorite, the undivided granitic rocks are significantly richer in potassium feldspar and, locally, display a well-developed protoclastic texture. The age of these rocks is not known, but they are tentatively assigned the same age as the Fadliyah granodiorite.

QUARTZ MONZONITE (qm)

The southwest corner of the quadrangle is underlain by medium- to coarse-grained quartz monzonite that is lighter colored and more recessive weathering than the adjacent undivided granite. The contact between the two is convex away from the quartz monzonite, which suggests that the adjacent undivided granite is older. However, the age of the quartz monzonite relative to the Darb Zubaydah ophiolite and the other granitic rocks in the quadrangle is not constrained.

SAKHIRAH GRANITE (sg)

The type locality of the Sakhirah granite is at Jabal Sakhirah in the north-central part of the quadrangle. It weathers to a red color, underlies low plains and scattered inselbergs, and ranges in composition from alkali-feldspar granite to syenogranite. The granite is composed of a fine- to medium-grained (0.1-2 mm) intergrowth of quartz, microcline, and minor amounts of plagioclase, biotite, and opaque minerals. The Sakhirah granite intrudes microgabbro of the Darb Zubaydah ophiolite and quartz diorite of the Umayrah complex; its age relative to the other post-ophiolite intrusive rocks is not known. It is, however, considered to be younger than the Saq'ah quartz diorite, Nifazi granite, and Fadliyah granodiorite because of its more evolved composition.

Foliated Member (afgf)

Foliated alkali-feldspar granite crops out east of the Sakhirah granite. It is medium-grained, red weathering, and is distinquished from the Sakhirah granite only by a well-developed concentric foliation that appears to have developed in a protolith of Sakhirah granite during the forceful emplacement of a younger granodiorite pluton (see Foliated Granodiorite).

FOLIATED GRANODIORITE (gdf)

A single foliated granodiorite pluton crops out east of Jabal Saq'ah; it is light gray and has a protoclastic overprint on a primary porphyritic texture. Foliation is concentric and concordant with foliation in the foliated alkali-feldspar granite, metadiabase, and metagabbro, suggesting that deformation of these rocks occurred during emplacement of the granodiorite.

ALKALI GRANITE (ag)

A small alkali-granite pluton intrudes the Sakhirah granite north of Jabal Sakhirah; it is leucocratic, sugary textured, and foliated and lineated near its contact with the Sakhirah granite. It is

composed of a fine-grained (>0.3 mm) graphic-granular to graphic intergrowth of quartz, microcline/minor biotite, aegirine, and opaque minerals. Foliation and lineation suggest forcible emplacement in the Sakhirah granite.

ALKALI-FELDSPAR GRANITE (afg)

Small plutons and plugs of alkali-feldspar granite intrude the Fadliyah granodiorite, the volcanic and hypabyssal rocks of the Darb Zubaydah ophiolite, and the Saq'ah quartz diorite. The alkali-feldspar granite weathers brick red and is composed of a hypidiomorphic to protoclastic intergrowth of quartz, microcline, minor sodic plagioclase, opaque minerals, and minor biotite.

GRANOPHYRE (gph)

The alkali-feldspar granite grades into brick-red aphanitic granophyre with decreasing grain size. Granophyre plugs and dikes intrude the Darb Zubaydah ophiolite and other granitic rocks in the quadrangle, indicating that the granophyre and alkali-feldspar granite were emplaced late in the magmatic evolution of the Bi'r Nifazi area.

SANAM GRANITE (gs)

The Sanam is an alkali granite underlying Jabal Sanam; it is medium-grained and has a purple cast. It is composed of a medium-grained (0.3-3 mm) intergrowth of quartz, microcline, biotite, sphene(?), and minor plagioclase and arfvedsonite. South of the quadrangle, it contains peridotite roof pendants of the Darb Zubaydah ophiolite. Its age is poorly constrained relative to the other granite of the quadrangle, but its highly evolved composition suggests it is relatively young.

POST-OPHIOLITE SEDIMENTARY ROCKS AND DEPOSITS

JIBALAH GROUP

Sedimentary rocks of the Jibalah group (Delfour, 1977) underlie small areas along the trace of the major northwest-striking Najd fault in the south-central part of the quadrangle. These rocks were apparently deposited in small grabens formed during faulting on the Najd fault system. Their age is poorly constrained within the Bi'r Nifazi quadrangle, but regionally they are considered to be lower-most Paleozoic or upper-most Proterozoic in age (Delfour, 1977, 1981).

Conglomerate (jc)

Conglomerate underlies a low ridge southwest of Jabal al Ghirah; it is a clast-supported aggregate of well-rounded cobbles and boulders with a matrix of poorly indurated sandstone. Boulders and cobbles consist of medium-grained granodiorite, coarse-grained alkali-feldspar granite, granophyre, and very fine-grained gabbro, in order of decreasing abundance. The presence of clasts of alkali-feldspar granite and granophyre indicate that this unit was probably deposited after all or most of the plutonic rocks in the quadrangle were emplaced, uplifted, and eroded.

Limestone (jm)

Well-bedded brown limestone overlies undivided granite south of Jabal al Ghirah. Beds range in thickness from a few centimeters to about 1 m and were warped into broad, open folds.

QUATERNARY DEPOSITS

Terrace Gravel (Qt)

Remnants of terrace-gravel deposits are preserved between Jabal Aftah and Wadi al Umayrah. The deposits are less than 3 m thick and rest on a paleoweathering horizon. They are composed of locally derived angular clasts in a soft, clay-rich matrix. The age of these deposits was not determined, but is inferred to be Pleistocene.

Fan Deposits (Qf)

Remnants of ancient fan deposits are preserved on the east flank of Jabal Aftah. They are not indurated and appear to be "fossil" deposits, as they are covered with a thick desert varnish and are dissected by active stream channels.

Playa Lake Deposits (Qp)

White- to tan-colored clay and silt deposits underlie playa lakes that formed in small enclosed basins throughout the quadrangle.

Surficial Deposits, Undivided (Qu)

Alluvium, colluvium, modern fan deposits, and wind-blown deposits of sand, silt, and clay are collectively mapped as undivided surficial deposits.

METAMORPHISM

Rocks of the Darb Zubaydah ophiolite are pervasively altered to greenschist-facies assemblages; relicts of primary mafic minerals are extremely scarce and plagioclase has been extensively albitized. The primary minerals of the ultramafic rocks were completely replaced by serpentine, talc, and carbonate minerals. Intense carbonate metasomatism obliterated primary mineralogy, textures, and structures. Amphibolite-facies assemblages are developed in roof pendants within narrow (< 30 m) aureoles around the Umayrah complex and Nifazi granite.

GEOCHEMISTRY

This investigation focuses on the geochemistry of the Darb Zubaydah ophiolite. No attempt has been made to characterize the compositions of intrusions that clearly postdate the ophiolite.

GEOCHEMICAL TECHNIQUES

Whole-rock analyses were performed by electron microbeam analysis (EMA) of glass beads to obtain major-element abundances, and by X-ray fluorescence (XRF) spectroscopy of compacted powder to obtain trace-element abundances. Each sample was crushed and ground to 200 mesh. A split of the resulting powder was melted to form a glass bead for EMA and a second split was compacted for XRF analysis. Glass beads were produced by melting powder suspended on platinum loops in a vertical furnace open to the atmosphere. Basalt and andesite samples were heated to approximately 1,300°C for 3 hours and rhyolite samples were heated to approximately 1,100°C for 3 hours. Quenching was performed with a compressed-air gun. Glasses were ground and remelted to optimize homogeneity. Volatiles (F, Cl, H_2O and CO_2) are lost during glass preparation so that EMA analyses are the volatile-free equivalent of the original sample composition. Analysis of 20 USGS and international rock standards indicates that sodium and potassium do not appear to be affected by glass preparation or analysis (J.E. Quick and M.A. Hussein, unpublished data).

EMA was performed on mineral grains and polished-glass mounts using a JEOL T300 scanning electron microscope (SEM) equipped with a Tracor Northern Si(Li) energy dispersive X-ray detector (EDA). Operating conditions were 15 kV accelerating potential and a take-off angle of 25°.

The XRF analysis was performed using a Kevex 7000 X-ray fluorescence analyzer interfaced to an IBM-PC. Samples were excited at atmospheric pressure using ^{109}Cd and ^{241}Am radioactive sources. X-ray spectra were collected using a Kevex Si(Li) EDA and transferred to an IBM-PC for analysis and storage. Spectral analysis was performed using XAP, a least-squares spectral deconvolution program (Quick and Helaby, 1988).

The data are presented in Appendix A (Table 2) and are considered to be fully quantitative for major elements determined by EMA and semiquantitative for trace elements determined by XRF. Absolute accuracy for the EMA results was found to be 2-5 percent of the abundance for elements present in greater than 1 percent abundance, based on analysis of rock standards with published compositions (J.E. Quick and M.A. Hussein, unpublished data). Absolute accuracy for the XRF depends on the abundance of the element and on which X-ray lines (K, L, or M) are measured; 5 to 15 percent of the abundance is presently the best accuracy obtainable on this system (Quick and Helaby, 1988).

RESULTS

The data are presented graphically in figures 3-10 (shown at the end of section, starting on page 18). In addition to the data in Appendix A, these figures include data published by Quick and Bosch (1989) for the Darb Zubaydah ophiolite.

The extensive greenschist-facies alteration and local carbonate metasomatism of the rocks analyzed in this study suggest that the original rock compositions may have been modified significantly. To minimize the effect of carbonate metasomatism, rocks obviously affected by metasomatism were not analyzed and rocks with greater than 13 weight percent CaO, a conservative upper limit for unaltered volcanic rocks, were omitted from the diagrams. Nevertheless, sodium and potassium concentrations are particularly suseptible to modification by low-grade metamorphic processes, and conclusions drawn from them in greenschist terranes must always be carefully evaluated.

CHEMICAL SUITES

Extensive alteration of the ophiolitic rocks has obscured many of the chemical fingerprints that might otherwise be used to identify groups of chemically related rocks. Nevertheless, the volcanic, hypabyssal, and plutonic rocks of the ophiolite can be tentatively grouped into three suites of chemically similar rocks (figs. 3-6). First, the massive tuff and welded tuff have similar calc-alkaline affinities and are interpretted to belong to the same suite. The plutonic equivalents of the welded tuff may be represented by the Zaynah granodiorite and Baraq quartz diorite. Second, a strong case can be made for a consanguineous relationship between the upper basalt and the diabasic rocks and the gabbro and micro-gabbro may be cumulate-rich rocks of the same suite. Third, the lower basalt appears to represent a distinct suite for which there is no identifiable intrusive equivalent.

Figure 3 displays plots (organized by map unit) of FeO versus FeO/MgO for volcanic and intrusive rocks of the Darb Zubaydah ophiolite. Massive tuff and welded tuff (fig. 3A) show considerable scatter but define a weak FeO-depletion trend with increasing FeO/MgO, suggesting a calc-alkaline affinity. The trends with the most similarity among the intrusive rocks are exhibited by the Zaynah granodiorite and Baraq quartz diorite (fig. 3 D), which display weak FeO depletion to constant FeO with increasing FeO/MgO. The upper basalt (fig. 3B) is characterized by considerable scatter, but data define an Fe-enrichment trend with increasing FeO/MgO. This contrasts with the calc-alkaline trend of the massive and welded tuffs, and suggests that the upper-basalt magmas evolved by fractional crystallization of pyroxene and(or) olivine. Similar (and overlapping) Fe-enrichment trends are defined by the data for the diabasic rocks (fig. 3 E) and the gabbro and microgabbro (fig. 3F), which suggests that those rocks may be the intrusive equivalents of the upper basalt group. In marked contrast, rocks of the lower basalt group (fig. 3C) define an Fe-depletion trend with increasing FeO/MgO, which suggests a calc-alkaline affinity, and does not overlap with the compositional field of any of the intrusive rocks.

Figure 4 displays plots of TiO_2 versus FeO/MgO for volcanic and intrusive rocks. Massive and welded tuff (fig. 4A) collectively define a field showing a weak TiO_2-depletion trend with increasing FeO/MgO. Similar trends are displayed by the Zaynah granodiorite and Baraq quartz diorite (fig. 4 D). The upper basalt is characterized by a distinctive, strong TiO_2-enrichment trend. Data for the diabase and diabase porphyry (fig. 4E) define a similar overlapping trend, reinforcing the impression that these rocks are consanguineous with the upper basalt. The gabbro and microgabbro (fig. 4F) data cluster at the low-TiO_2 end of the Fe-enrichment trend, suggesting that the gabbroic rocks could be related cumulate-rich rocks. The lower basalt sequence is characterized by a TiO_2-depletion trend that has no analog, except among significantly younger tuffs of the ophiolite.

Figure 5 displays plots of SiO_2 versus FeO/MgO for the volcanic and intrusive rocks. The massive tuff and welded tuff (fig. 5A) show considerable scatter but are characterized by a poorly defined SiO_2-enrichment trend. The field defined by the Zaynah granodiorite and Baraq quartz diorite (fig. 5D) is similar to that of the welded tuff, suggesting that the former may be plutonic equivalents of the latter. In contrast, the upper basalt data do not display a well-defined SiO_2-enrichment trend. This field is similar to fields defined by the gabbro (fig. 5F) and the diabase (fig. 5E), although the diabase data displays a slight SiO_2-enrichment trend. The lower basalt is characterized by a strong SiO_2-enrichment trend, which, again, has no analog among the intrusive rocks.

Figure 6 illustrates the compositonal variations in the welded tuff, Zaynah granodiorite, and Baraq quartz diorite for well-analyzed oxides and elements that are, with the exception of SiO_2, relatively immobile during low- to moderate-grade metamorphism. The similarity in fields defined by these plutonic rocks and tuffs reinforces the impression that they are cogenetic.

ERUPTIVE ENVIRONMENT

Figures 7 through 10 are diagrams commonly used to infer the eruptive environment of volcanic rocks. Except for figure 8, these diagrams focus on elements that are considered to be relatively immobile during low- to moderate-grade metamorphism. The fields defined in most of these diagrams are based on the assumption that analyzed rocks are extrusive and represent true melt compositions. Therefore, hypabyssal and plutonic rocks of the ophiolite are included in these diagrams only for comparison to the volcanic rocks.

Figure 7 displays the compositions of Darb Zubaydah basaltic, diabasic, and gabbroic rocks on the MgO-FeO-Al_2O_3 ternary diagram of Pearce and others (1977). With few exceptions, the basaltic rocks (fig. 7A, B, and C) plot in the island-arc basalts field. Similarly, compositions of three out of four diabase-porphyry samples (fig. 7D) plot in the island-arc basalt field. The diabase, microgabbro, and gabbro data (fig. 7D and E), however, plot in the continental basalts, ocean-floor basalts, and ocean-island basalts fields. This is interpreted to reflect the presence of a cumulate component (olivine, pyroxene, or amphibole) in these rocks, which would tend to enrich their compositions in FeO and MgO relative to Al_2O_3.

Figure 8 presents AFM diagrams for the volcanic and intrusive rocks of the Darb Zubaydah ophiolite. The volcanic rocks (fig. 8A, B, and C) collectively define an elongate field that crosses from the tholeiitic region to the calc-alkalic region of the diagram. Relatively evolved alkali-rich rocks are abundant in the massive and welded tuffs (fig. 8A), and are present, to a lesser extent, in the lower basalt (fig. 8C). The upper basalt data (fig. 8B) plots in more alkali-depleted regions than either the lower basalt data (fig. 8C) or the massive and welded tuffs (fig. 8A); this could reflect extreme alkali loss in the more altered rocks of the upper basalt or the presence of more primitive basalts in that unit. The Zaynah granodiorite and the Baraq quartz diorite (fig. 8D) plot near the most alkali-enriched part of the trend defined by volcanic rocks, possibly reflecting an increase in alkali content produced by alteration (as evidenced by secondary muscovite). Most analyses of diabase, diabase porphyry, microgabbro, and gabbro (fig. 8E and F) cluster in the tholeiitic region at the low-alkali end of the field defined by volcanic rocks. The field defined by these hypabyssal and plutonic rocks is consistent with preceding evidence that they may represent cumulates and cumulate-rich melts that are related to the mafic volcanic rocks through fractional crystallization.

The TiO_2 and zirconium abundances (fig. 9) are considered relatively insensitive to greenschist-facies metamorphism and, therefore, are useful for distinguishing altered basalts that formed in different tectonic environments (Pearce, 1979). Consistent with stratigraphic and major-element (fig. 7) evidence, basaltic-composition rocks from the massive tuff and welded tuff units (fig. 9A) and the lower basalt (fig. 9C) plot entirely within the intersection of the fields defined by island-arc and mid-ocean ridge basalts. In contrast, the upper basalt data (fig. 9B) defines a field that extends to very high TiO_2 abundances (3.5 percent) and closely matches that defined by mid-ocean-ridge basalts. Therefore, these data indicate the presence of two geochemically distinct groups of basalts, high-TiO_2 and low-TiO_2, within the ophiolite. However, as will be discussed later, the data does not necessarily indicate the presence of a mid-ocean-ridge component. Diabase and diabase-porphyry compositions (fig. 9D) define a field that is similar to the field defined by the upper basalt sequence, reinforcing the impression of a

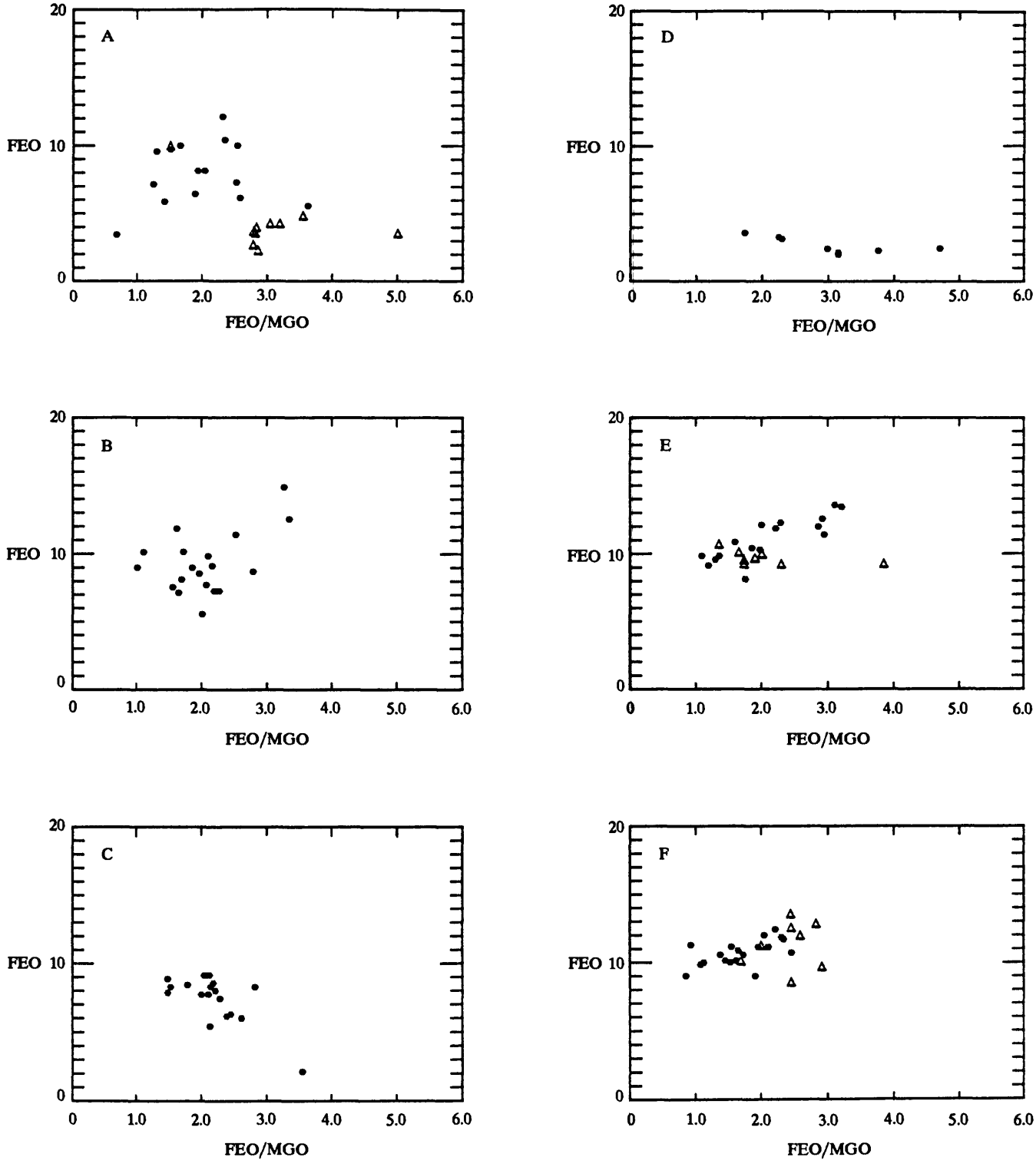

Figure 3.– Diagrams showing FeO vs. FeO/MgO for volcanic and hypabyssal rocks of Darb Zubaydah ophiolite: (A) massive tuff (dots) & welded tuff (triangles); (B) upper basalt sequence; (C) lower basalt sequence; (D) Baraq quartz diorite, felsite and Zaynah granodiorite; (E) diabase (dots) & diabase porphyry (triangles); and (F) gabbro (dots) & microgabbro (triangles). Total iron expressed as FeO.

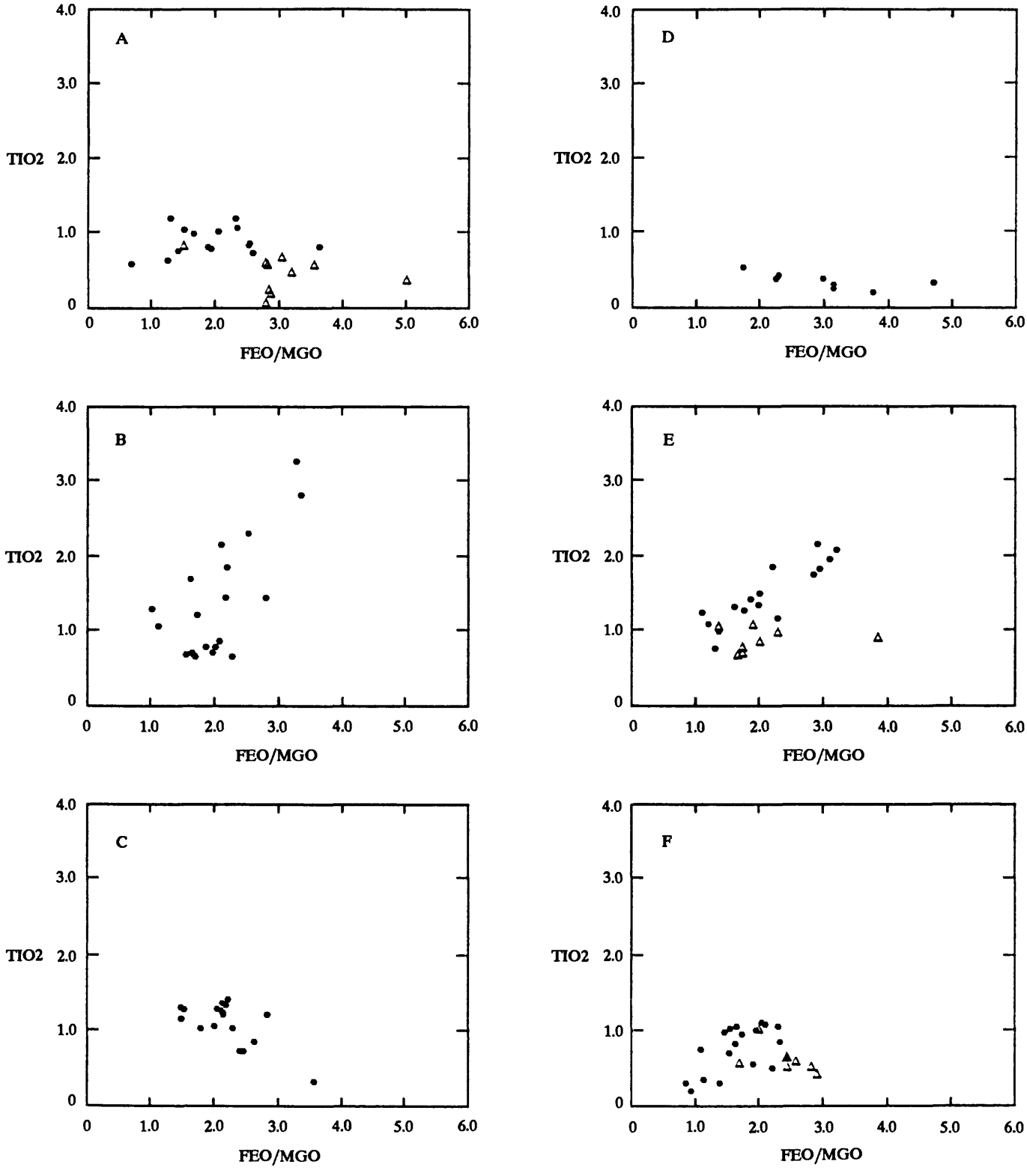

Figure 4.-- Diagrams showing TiO_2 vs. FeO/MgO for volcanic and hypabyssal rocks of Darb Zubaydah ophiolite: (A) massive tuff (dots) & welded tuff (triangles); (B) upper basalt sequence; (C) lower basalt sequence; (D) Baraq quartz diorite, felsite and Zaynah granodiorite; (E) diabase (dots) & diabase porphyry (triangles); (F) gabbro (dots) & microgabbro (triangles). Total iron expressed as FeO.

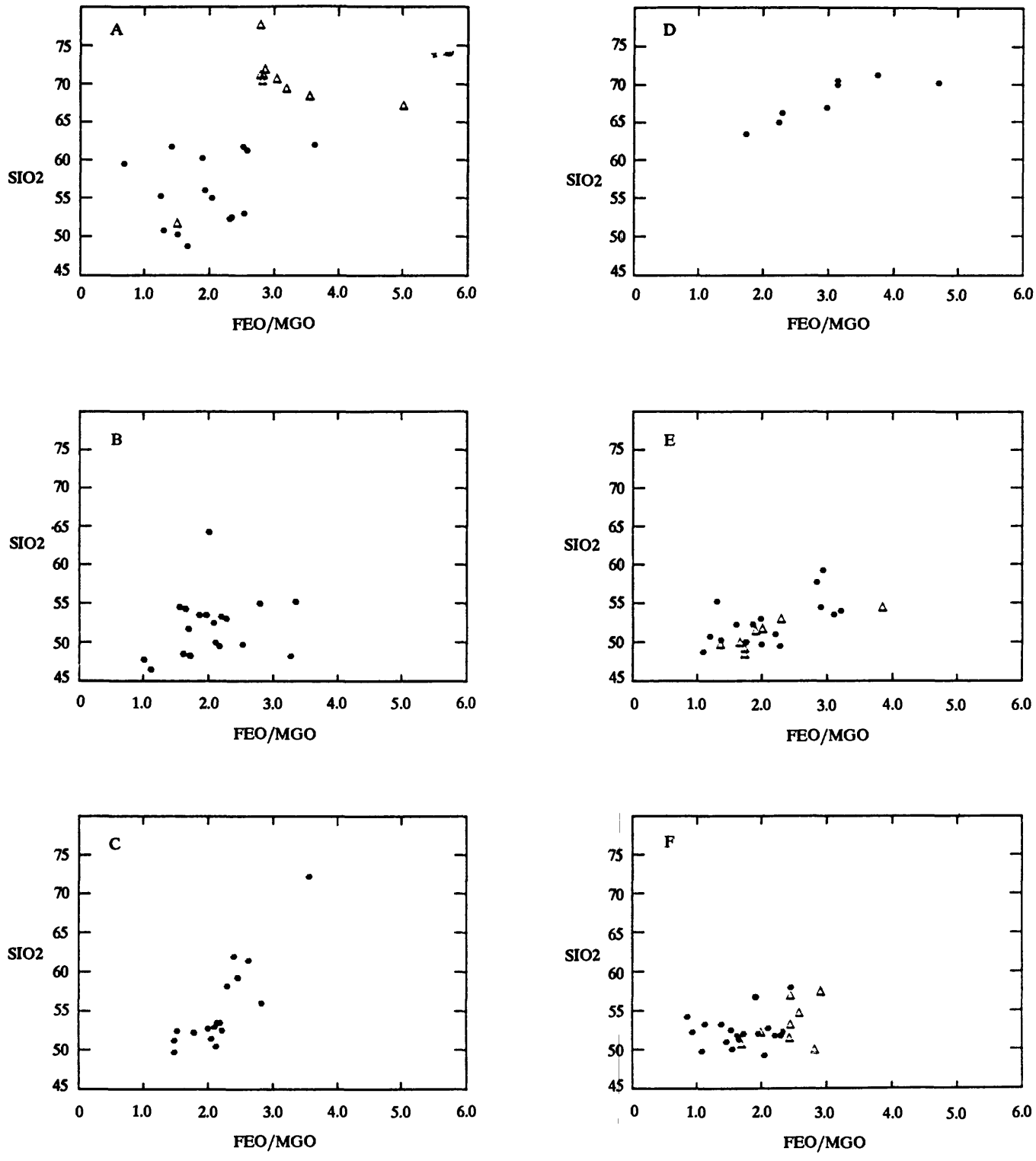

Figure 5.-- Diagrams showing SiO_2 vs. FeO/MgO for volcanic and hypabyssal rocks of Darb Zubaydah ophiolite: (A) massive tuff (dots) & welded tuff (triangles); (B) upper basalt sequence; (C) lower basalt sequence; (D) Baraq quartz diorite, felsite & Zaynah granodiorite; (E) diabase (dots) & diabase porphyry (triangles); and (F) gabbro (dots) & microgabbro (triangles). Total iron expressed as FeO.

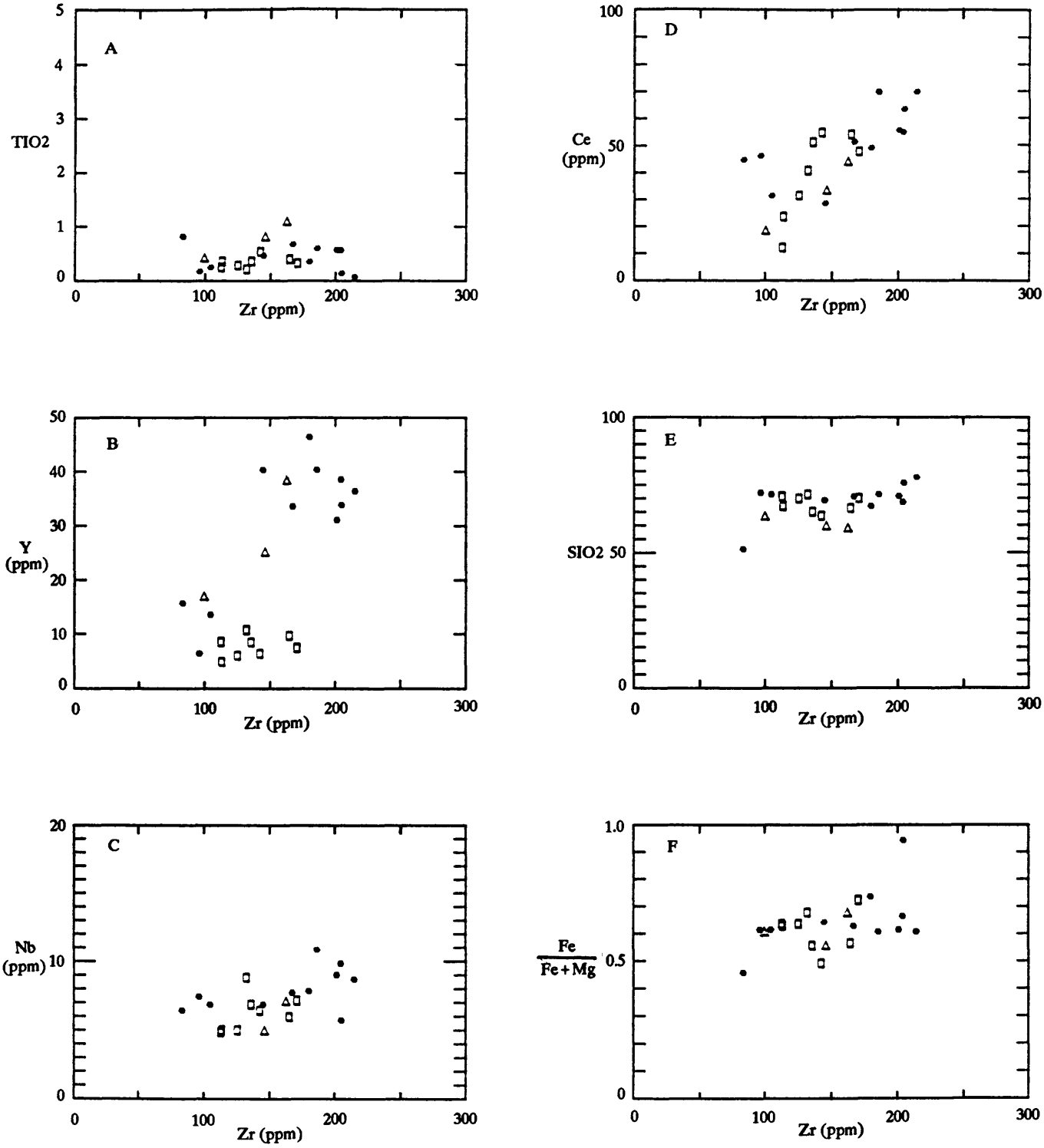

Figure 6.– Diagrams showing abundance of TiO_2, Y, Nb, Ce, and SiO_2 & Fe/Fe+Mg as a function of Zr abundance in welded tuff (dots), Zaynah granodiorite (squares), and Baraq quartz diorite & felsite (triangles). Total iron expressed as Fe.

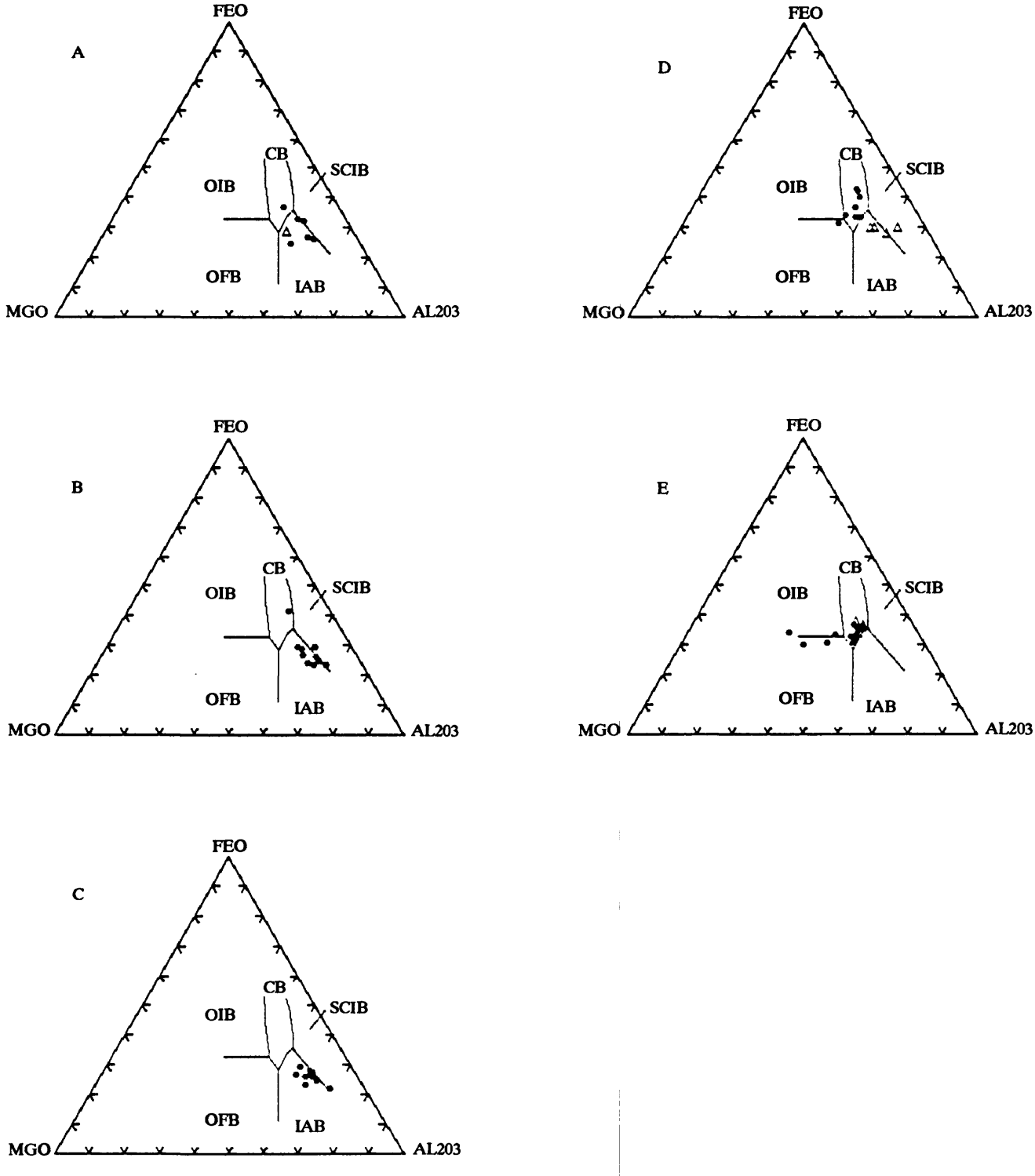

Figure 7.-- MgO-FeO-Al_2O_3 ternary diagrams for volcanic and hypabyssal rocks of Darb Zubaydah ophiolite: (A) massive tuff (dots) & welded tuff (triangles); (B) upper basalt sequence; (C) lower basalt sequence; (D) diabase (dots) & diabase phyry (triangles); (E) gabbro (dots) & microgabbro (triangles). Fields defined by Pearce and others (1977): IAB, island-arc basalts; OFB, oceanfloor basalts; OIB, ocean-island basalts; CB, continental basalts; SCIB, spreading-center-island basalts

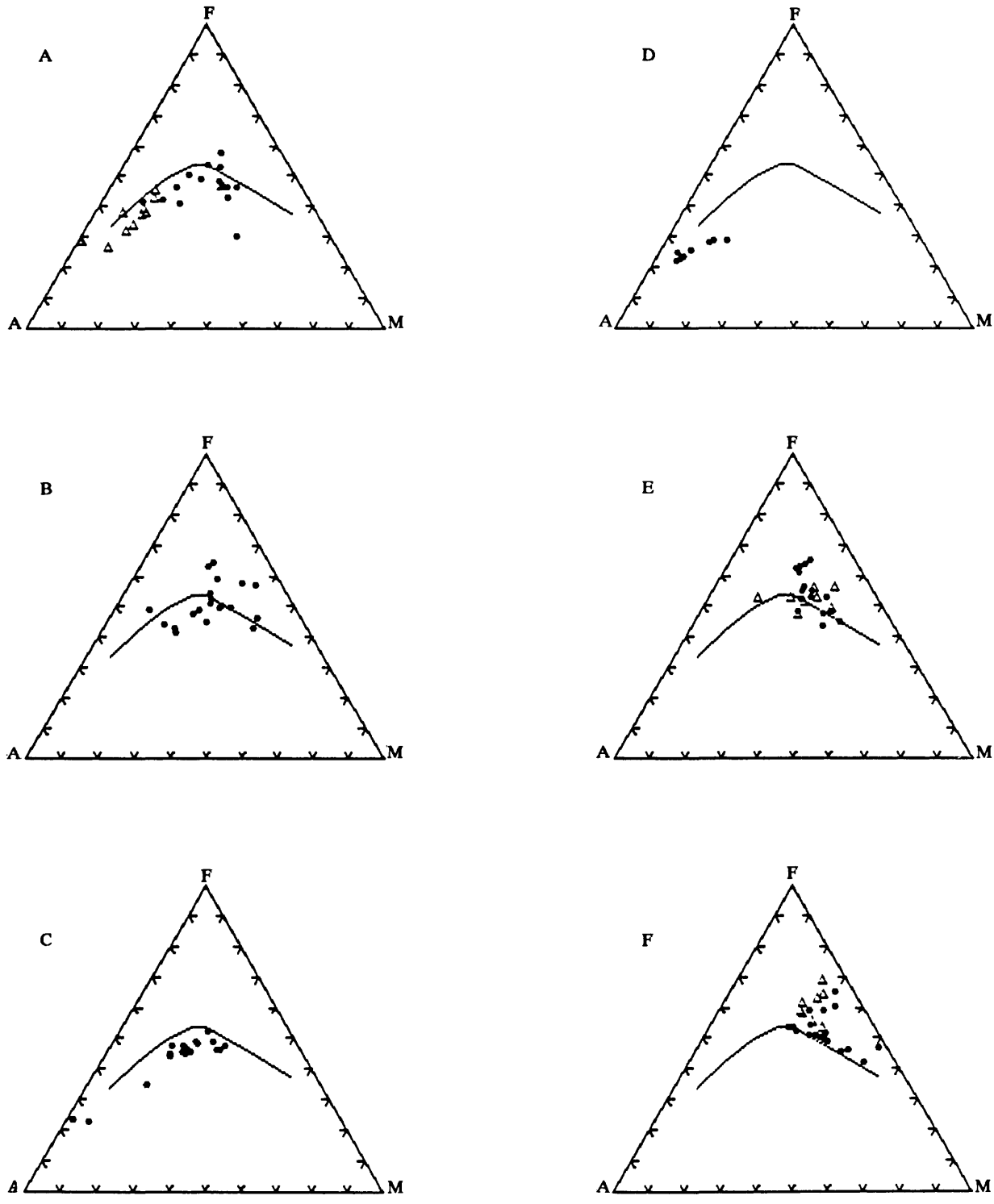

Figure 8.-- AFM ternary diagrams for volcanic and hypabyssal rocks of Darb Zubaydah ophiolite: (A) massive tuff (dots) & welded tuff (triangles); (B) upper basalt sequence; (C) lower basalt sequence; (D) Baraq quartz diorite, felsite & Zaynah granodiorite; (E) diabase (dots) & diabase porphyry (triangles); (F) gabbro (dots) & microgabbro (triangles). Curved line separates fields defined by Irvine and Baragar (1971) for tholeiitic rocks (above) from calc-alkaline rocks (below).

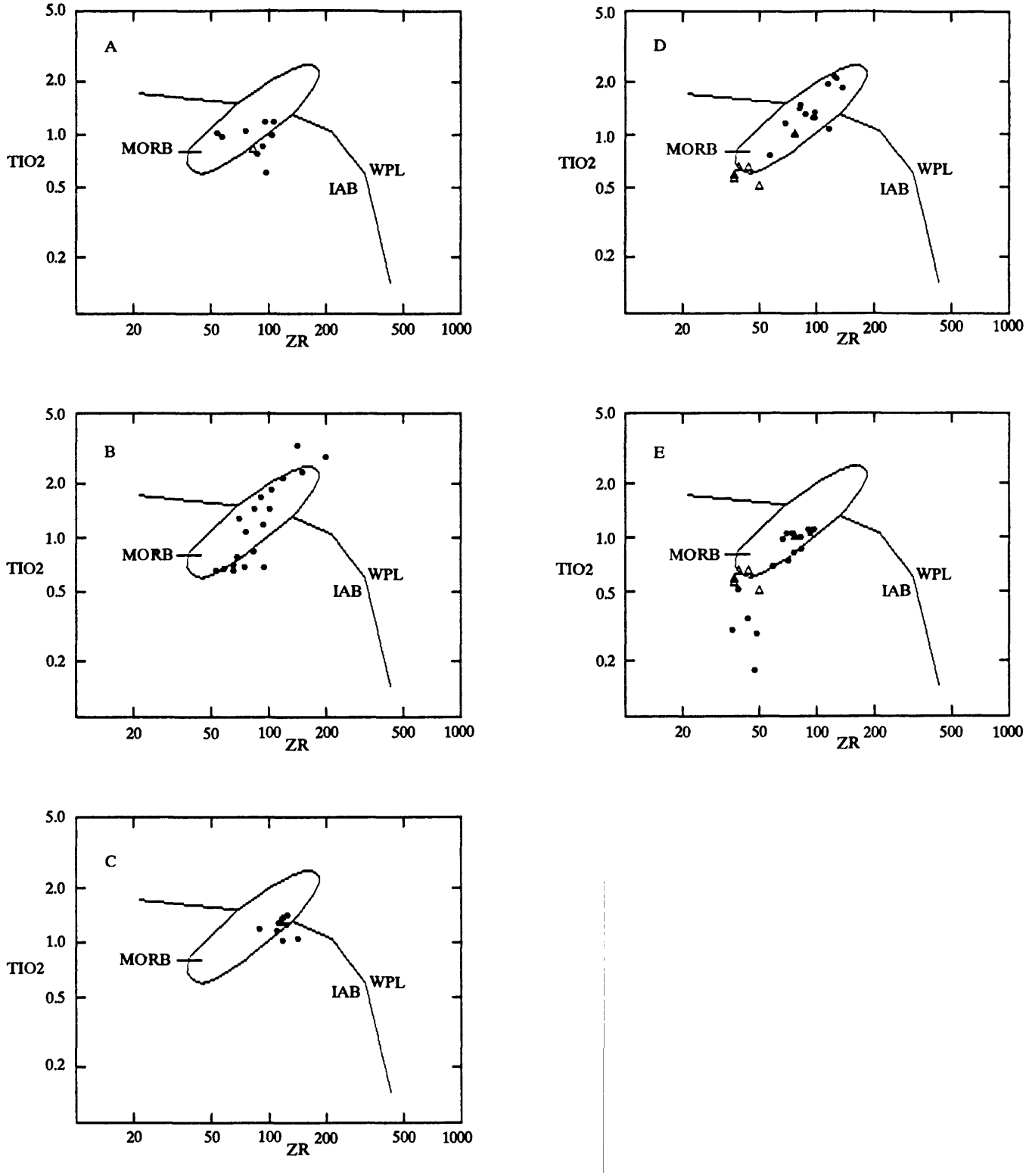

Figure 9.-- Diagrams showing TiO_2 versus Zr for volcanic and hypabyssal rocks of Darb Zubaydah ophiolite: (A) massive tuff (dots) & welded tuff (triangles); (B) upper basalt sequence; (C) lower basalt sequence; (D) diabase (dots) & diabase por-phyry (triangles); (E) gabbro (dots) & microgabbro (triangles). Fields as defined by Pearce (1979): IAB, island-arc basalts; MORB, midocean ridge basalts; WPL, within-plate basalts.

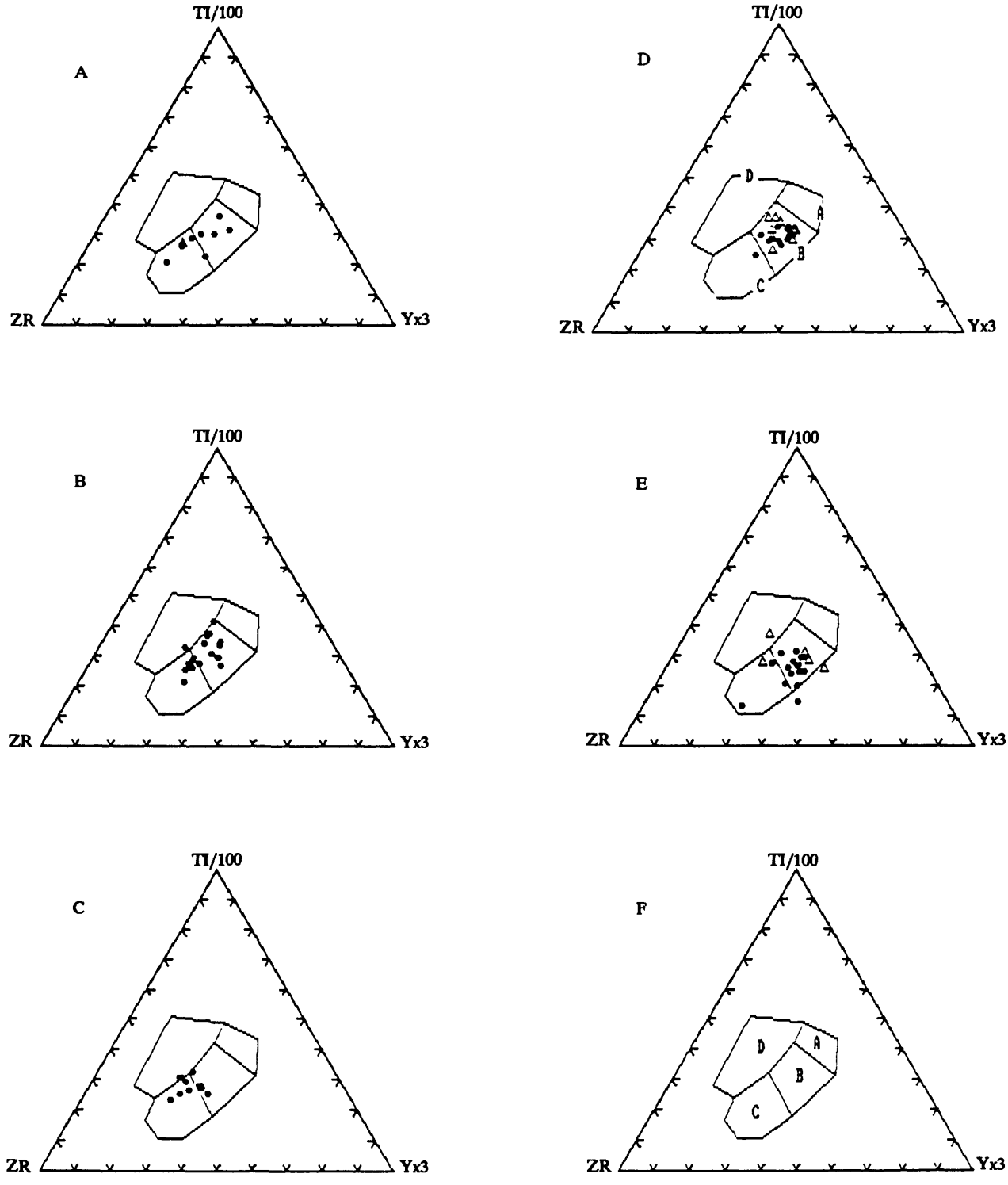

Figure 10.– Zr-Ti-Y ternary diagrams for volcanic and hypabyssal rocks of Darb Zubaydah ophiolite: (A) massive tuff (dots) & welded tuff (triangles); (B) upper basalt sequence; (C) lower basalt sequence; (D) diabase (dots) & diabase porphyry (triangles); (E) gabbro (dots) & microgabbro (triangles); (F) key to identifying fields defined by Pearce & Cann (1973): oceanic-island basalts, D; ocean-floor basalts, B; low-K tholeiites, A and B; calcalkali basalts, C and B.

consanguineous link between these units. The gabbro and microgabbro compositions plot within the island-arc-basalt field; their low abundances of titanium and zirconium relative to the volcanic rocks are consistent with the presence of a significant cumulate component.

Figure 10 displays zirconium-titanium-yttrium ternary diagrams for basaltic-composition rocks of the Darb Zubaydah ophiolite. Virtually all of the basalts (fig. 10A, B, and C) and basaltic-composition intrusive rocks (fig. 10D and E) plot within the calc-alkali basalts fields.

Figures 7 through 10 illustrate that most of the basaltic-composition volcanic rocks have compositions consistent with eruption in an island-arc environment. The high-TiO_2 basalts of the upper basalt sequence appear to be a significant complication. Shervais and Kimbrough (1985) describe two basaltic suites (high-TiO_2 and low-TiO_2, in the Coast Range ophiolite of California and conclude that the Coast Range ophiolite is composed of crust formed in an island-arc setting (low-titanium), and crust formed in a mid-ocean-ridge or oceanic-island setting (high-titanium). However, the contrasting suites in california are separated by tens to hundreds of kilometers, whereas, in the Darb Zubaydah ophiolite, high- and low-titanium basalts are part of the same volcanosedimentary pile and probably erupted from coeval, closely spaced but distinct vents. It is suggested that the low-titanium basalts were normal island-arc tholeiites. High-titanium basalts may have been erupted during an episode of intra-arc rifting or may have been erupted from a volcanic source similar to the Esmeralda Banks, a volcanic center characterized by high-titanium basalts and located behind the main Mariana volcanic arc (Stern and Bibee, 1984).

GEOCHRONOLOGY

The only radiometric age available in the Bi'r Nifazi quadrangle is a Rb-Sr age (581 ± 6 Ma) determined for the Jabal Sanam granite (Delfour, 1981).

No radiometric-age data are available for the Darb Zubaydah ophiolite. However, rhyolitic tuff from the Nuqrah belt near the village of Nuqrah (fig. 2) has been dated at 839 ± 23 Ma by the U-Pb method and 821 ± 48 Ma by the Rb-Sr method (Calvez and others, 1983). These dates are thought to be the approximate age of the Darb Zubaydah ophiolite because the Nuqrah belt contains similar sedimentary and volcanic rocks and is continuous along strike from the type locality at Nuqrah to Bi'r Nifazi.

STRUCTURE

BATHOLITHIC STRUCTURES

Three quarters of the Bi'r Nifazi quadrangle is underlain by granitic rocks. The largest granitic mass, the Fadliyah granodiorite, is part of the Abu Salim granitic domain (fig. 2; Delfour, 1981), a composite batholith that extends 25 km to the west, more than 50 km to the south, and more than 50 km to the north. The center of the quadrangle is underlain by the northerly elongate Umayrah complex. The eastern quadrant of the quadrangle is underlain by Saq'ah quartz diorite and Nifazi granite, which are part of the Umm ash Shatun granite domain (fig. 2; Delfour, 1981) that extends more than 25 km to the east.

The Darb Zubaydah ophiolite is preserved as roof pendants within and as septa between these granitic batholiths. The ultramafic and gabbroic rocks at Jabal Aftah form a septum between the Fadliyah granodiorite and the Umayrah complex. Farther east, ophiolitic hypabyssal and volcanic rocks form a septum between the Umayrah complex, the Nifazi granite, and the Saq'ah quartz diorite. West and south of the quadrangle, roof pendants of ophiolitic rocks occur in the Abu Salim granitic domain (fig. 2) and constitute the country rocks into which the western margin of the Abu Salim granitic domain was intruded (fig. 2; Quick and Bosch, 1989)

FOLDING

The regional distribution and orientation of fragments of the Darb Zubaydah ophiolite suggest that the ophiolite was bowed into a 25-km wide, north-trending anticlinorium during the emplacement of the Fadliyah granite. Within the Bi'r Nifazi quadrangle, the two septa of ophiolitic rocks appear to be relicts of a steeply dipping homocline that exposes progressively deeper and older rocks toward the west. Exposures of the deepest ophiolitic rocks are found 5 to 10 km west of the Bi'r Nifazi quadrangle where tectonized peridotite forms roof pendants in the Abu Salim granitic domain (fig. 2). Farther west, a homoclinal section of the Darb Zubaydah ophiolite is exposed on the western margin of the Abu Salim granitic domain (fig. 2); this section exposes deeper crustal levels to the east and represents the west flank of the anticlinorium.

Although volcanic and sedimentary rocks are locally overturned to the west, the general lithologic sequence and sedimentary structures in tuffs and sandstones indicate that stratigraphic up is to the east, which is consistent with the direction indicated by the ophiolitic "stratigraphy". Apart from small, tight to isoclinal folds associated with faults and the homoclinal tilting of the ophiolitic section, there is no evidence of significant folding.

ZAYNAH GRANODIORITE EMPLACEMENT

There is evidence that the Zaynah granodiorite may have been emplaced as a thick sill within the Darb Zubaydah ophiolite before the section was rotated into a homocline. Chemical data suggest that the Zaynah granodiorite could be the plutonic equivalent of the welded tuff. This would require that the Zaynah granodiorite was emplaced during the evolution of the volcano-sedimentary pile of the ophiolite. Microgranodiorite chilled-margins and dikes are only found on the eastern side of the the Zaynah pluton implying, that the top of the pluton is now its eastern flank. This suggests that the pluton was rotated about 90° since emplacement.

THRUST FAULTS

A single thrust fault placed serpentinite over gabbro along the southern side of Jabal Aftah. The thrust dips 40° to the northwest and its northeast strike suggests that it formed in response to northwestward directed compression. However, the age of movement on the fault is constrained only to be prior Najd faulting, and it is possible that the fault is, in fact, a normal fault that was rotated during homoclinal tilting of the ophiolite.

GHAYHAB FAULT

The Ghayhab fault consists of a north-trending swarm of anastomosing faults that parallel Wadi Ghayhab and extend northward through Jabal Mardah. Individual strands of the fault are identified by foliated to mylonitized rock that grade into the less-deformed rocks that flank the strands. Ghayhab faulting appears to have been most intense in the Kaffan sandstone, but also involved the overlying volcanic rocks and underlying diabase. Carbonate replacement is locally extreme within the deformed rocks. Individual strands are about 200 m wide and contain abundant lenses of less-deformed rock. Small, isoclinal folds and complex refolded folds are present along the margins of some of the less-deformed lenses. A left-lateral sense of motion is indicated by (1) the presence of drag folds in carbonate layers within and near strands of the fault, (2) offset of the Zaynah granodiorite east of Wadi Ghayhab, and (3) offset on mappable beds and clinopyroxene-rich gabbro intrusions in the upper basalt sequence and massive tuff.

Ghayhab faulting appears to have been coincident with emplacement of the Zaynah granodiorite. Dikes of Zaynah micro-granodiorite intrude mylonite of the Ghayhab fault, but are broken into boudins and rotated into the plane of the Ghayhab fault in many places. The age and significance of both the Ghayhab fault and Zaynah granodiorite, however, are problematic.

Quick and Bosch (1989) previously considered the Ghayhab fault to be a high-angle, left-lateral fault of the north-trending Nabitah fault system. According to that model, major movement on the Ghayhab fault would have been about 100 m.y. younger than the formation of the Darb Zubaydah ophiolite. Examples of syntectonic intrusion of gabbro, diorite, and granodiorite are clearly visible along the main strand of the Nabitah fault system (Quick, unpublished maps). However, strike-slip faulting is inconsistent with evidence suggesting that the Zaynah granodiorite was emplaced late in the

evolution of the ophiolite at about the same time as major movement occurred on the Ghayhab fault.

Some characteristics of the Ghayhab fault and Darb Zubaydah ophiolite suggest that the Ghayhab fault formed as an ancient gravity slide within the evolving ophiolite, and that it was subsequently rotated into its present orientation during regional tilting of the ophiolite. First, the traces of many of the strands of the Ghayhab fault are arcuate, as in a gravity-driven rotational slide. Second, the Ghayab fault zone cuts progressively deeper into the volcanosedimentary section from Jabal Zaynah north to where the faults cross Wadi Ghayhab. From that point northward, many Ghayhab faults cut abruptly higher into the volcanosedimentary section. Third, given the above-mentioned geometry, offset of volcanosedimentary units by the Ghayhab could be normal slip southeast of Wadi Ghayhab and reverse slip northwest of Wadi Ghayhab. These characteristics do not provide a model for formation of the Ghayhab fault using north-directed gravity sliding of the volcanic and sedimentary rocks.

Uplift resulting from emplacement of the Zaynah granodiorite could have triggered large landslides on the flanks of the inflating pluton. Ductile sedimentary strata of the Kaffan sandstone and lahar deposits may have lubricated the downslope movement of the more rigid, overlying volcanic rocks. Although the hypothetical slide(s) would have been enormous (extending for a minimum 20 km in the postulated direction of sliding), slides of similar and even larger size have been documented on the submarine flanks of the Island of Hawaii (Lipman and others, 1988).

Najd Faulting

A system of steeply dipping, northwest-trending faults cuts the ophiolite and most of the younger plutonic rocks in the quadrangle. Motion on these faults involved a major component of left-lateral slip. Unlike the Ghayhab fault zone, deformation is concentrated in narrow, discrete zones. The orientation, age, and sense of motion of these faults is characteristic of the Najd fault system throughout the Arabian Shield (Schmidt and others, 1978). This system clearly offsets the Ghayhab fault in many places. Northwest-trending faults also offset small alkali-feldpar granite plutons and Nifazi granite that cut strands of the Ghayhab fault.

Northeast-Trending Faults

The quadrangle is also cut by several steeply dipping, northeast-trending faults. Offset on these faults appears to have involved a significant right-lateral component, suggesting that they may be conjugates of the northwest-trending Najd faults. However, the northeast-trending faults that cut the Fitar and Sifar gossans may have formed by normal slip while the ophiolite was evolving.

SYNTHESIS

A nearly complete, east-facing section of the Darb Zubaydah ophiolite is preserved in septa between large granitic plutons in the Bi'r Nifazi area. The lowest unit in the ophiolitic section within the quadrangle is composed of serpentinized ultramafic rocks of probable cumulate origin intruded by gabbro and diabase dikes. The serpentinite is in turn overlain by gabbro and microgabbro, diabase rocks, a lower basalt, a thick sandstone unit (the Kaffan sandstone), an upper basalt, and interbedded tuff, basalt, and sedimentary rocks. Gossans formed by the weathering of disseminated-sulfide deposits are interbedded with the pillow basalt and lahar deposits. Although tectonized peridotite, which represents the lowest structural unit of most ophiolites, is not present at the base of the Darb Zubaydah ophiolite, roof pendants of tectonized peridotite are present in the granodiorite batholith west of the Bi'r Nifazi quadrangle. Emplacement of large granitic plutons has rotated the entire ophiolitic section into a subvertical orientation.

The ophiolite appears to comprise the oldest rocks in the area; all plutonic rocks are either part of the ophiolite or intrude it. Reports of the presence of pre-ophiolitic basement rocks in the Bi'r Nifazi area (Delfour, 1981) are not supported by this investigation.

The abundance of pillow basalt, volcanic wacke, coarse-grained andesitic to rhyolitic tuff, and volcaniclastic rocks, and the absence of pelagic

sediments suggests that the Darb Zubaydah ophiolite formed in the vicinity of an island-arc (rather than at a spreading ridge or back-arc basin) and is, therefore, an example of the type-D ophiolite of Leitch (1984). The evolution of the ophiolite appears to have involved emplacement of abundant hypabyssal and plutonic rocks that intruded into progressively higher levels of the ophiolite. These intrusive rocks equaled or exceeded the volume of the associated volcanic rocks.

The composition of the lower basalt, the oldest extrusive unit in the ophiolite, ranges from island-arc tholeiite to andesite to keratophyre, suggesting that they formed in a young, relatively unevolved island arc. A thick, overlying section of wacke and lahar deposits was formed as a volcaniclastic apron adjacent to an active, volcanic arc during a period of local volcanic quiescence and basin subsidence. Extrusion of the overlying sequence of TiO_2-rich basalts and emplacement of voluminous consanguineous diabase suggests that the quiescent period was followed by an episode of intra-arc rifting. Extrusion of voluminous tuff may have accompanied emplacement of the Zaynah granodiorite and Baraq quartz diorite plutons. Landsliding, possibly triggered by emplacement of the Zaynah granodiorite and loading by voluminous tuffs, may have transported the upper part of the ophiolite northward and produced the Ghayhab fault zone.

ECONOMIC GEOLOGY

The Mardah gossans represent the only significant economic potential in the Bi'r Nifazi quadrangle. The size of these features and the presence of excellent conductors at depth (M. Bazzari, written communication, 1987) suggest that large sulfide deposits could be present. The three northernmost gossans, Shamal, Sifar, and Fitar, have been studied in detail. The geology, petrography, and chemistry of these gossans and their associated sulfides are described by Bosch and others (1989).

Chemical analysis of channel samples collected at right angles to the gossans indicates the presence of zones containing anomalously high nickel concentrations (1,000-10,000 ppm). Furthermore, there appears to be an increase in surface nickel concentrations north of the Fitar gossan at Jabal Mardah (<2,000 ppm), the Sifar gossan (5,000 ppm), and the Shamal gossan (10,000 ppm).

Reconnaissance drilling intersected sulfides beneath the Sifar and Fitar gossans but missed the sulfide zone beneath the Shamal gossan. The Sifar gossan is underlain by a steeply dipping, 15-to-25-m-thick, sulfide-rich volcanic wacke that contains nickel-rich (locally averages 1 percent) sulfides. The Fitar gossan is underlain by barren pyrite that is disseminated in sandstone, which is consistent with lower surface nickel concentrations.

The Mardah deposits appear to be compositionally and geologically unique. Unlike typical nickel-copper-sulfide deposits in ophiolites that occur near ultramafic rocks, the Mardah deposits occur high in the ophiolitic section and have low copper concentrations (<100 ppm). They are distinguished from the Bou Azzer cobalt-arsenide deposits of Morocco by their low arsenic abundances (typically <100 ppm) and high nickel-cobalt ratios (50:1). Compared to other nickel deposits (Naldrett, 1981), platinum-group element abundances are extremely low (<5 ppb). Furthermore, nickel-copper ratios at Jabal Mardah are extremely high, ranging from 150 to 250. In contrast, the nickel-sulfide deposits of Western Australia range from 10 to 65 (Marsten and others, 1981). Nickel-copper ratios reported by Naldrett (1981) for worldwide nickel deposits do not exceed 100.

ORE GENESIS

Additional work is required to construct an accurate ore-genesis model for Jabal Mardah. Available data suggest that the sulfides crystallized from hydrothermal solutions as they percolated through clastic rocks of the Kaffan sandstone and overlying lahar deposits. Pyrite, millerite (NiS), polydymite (Ni_3S_4), and minor sphalerite are interstitial to clasts of the wacke, and are intimately intergrown with quartz and nickel-rich epidote and chlorite. Ascending hydrothermal fluids may have been blocked by impermeable flows and tuffs, and forced to spread laterally in the more permeable underlying clastic rocks. In this model, the interlayered sulfide-rich and sulfide-poor layers

beneath the Fitar gossan formed by sulfide replacement along permeable strata rather than by deposition of sulfides directly on the ocean floor.

While an exhalative origin for the sulfides would require mineralization to occur during formation of the ophiolite, a hydrothermal-replacement origin requires only that mineralization be as old as or younger than the enclosing strata. However, sulfides may have been deposited before the ophiolitic section was rotated into a subvertical orientation. Pervasive alteration at the base of the upper basalt unit suggests that it was more strongly affected by hydrothermal circulation than the overlying rocks; this is consistent with confinement of hydrothermal circulation to the underlying sediments and would be most likely to occur if the upper basalt were subhorizontal during the hydrothermal event.

Nickel Source

The source of nickel in the Jabal Mardah deposits remains problematic. It is particularly perplexing in that the nickel-copper ratios (150 to 250) in these deposits greatly exceed those in other nickel-bearing deposits around the world; no mechanism, except supergene enrichment, is known that might concentrate economically significant amounts of nickel without also depositing substantial amounts of copper.

The serpentinized ultramafic rocks at Jabal Aftah are nickel-rich source rocks. However, it is unlikely that nickel was selectively leached from ultramafic rocks underlying mafic rocks several kilometers thick without leaching significant amounts of copper, lead, or zinc. It is also unlikely that unusual chemical conditions prevailed during mineralization at Jabal Mardah that would allow precipitation of nickel-rich sulfides and simultaneously restricted precipitation of copper, lead, and zinc sulfides. Alternatively, ultramafic rocks entrained in the Ghayhab fault may have been a source of nickel providing a high-nickel, low-copper, -lead, and -zinc source close to the ore bodies. However, ultramafic rocks are not known to exist in the Ghayhab fault within the Bi'r Nifazi quadrangle.

DATA STORAGE

All field and laboratory data for this report, including petrographic descriptions, sample sites, thin sections, field notebooks, and results of geochemical analyses, are stored in Data File USGS-DF-09-1 in the Jeddah office of the U.S. Geological Survey Saudi Arabian Mission. No updated information was added to the Mineral Occurrence Documentation System (MODS) data bank, and no new files were established.

REFERENCES

Anonymous, 1972, Penrose Field Conference on Ophiolites, report by conference participants: Geotimes, v.17, p. 24-25.

Bosch, P.S., Quick, J.E., Bazzari, M.A., Hussein, M.A., Helaby, A.M., Jannadi, Eyad, and Tayed, Jamal, 1989, Evaluation of the Jabal Mardah nickel prospect and geochemical survey of associated gossans, Kingdom of Saudi Arabia: Deputy Ministry for Mineral Resources Technical Record USGS-TR-09-4, 104 p., 2 plts., scale 1:5,000. USGS Open-file Report (in press)

Boudier, F., 1978, Structure and petrology of the Lanzo peridotite massif (piedmont Alps): Geological Society of America Bulletin, v.89, p. 1574-1591.

Brown, G.F., Layne, N.M., Jr., Goudarzi, G.H., and Maclean, W. H., 1963, Geologic map of the Northeastern Hijaz quadrangle, Kingdom of Saudi Arabia: U.S. Geological Survey Miscellaneous Geologic Investigations Map I-205-A, scale 1:500,000; reprinted 1979, Saudi Arabian Directorate General of Mineral Resources Geologic Map GM-205-A, scale 1:500,000.

Calvez, J. Y., Alsac, C., Delfour, J., Kemp, J., and Pellaton, C., 1983, Geologic evolution of western, central and eastern parts of the northern Precambrian Shield, Kingdom of Saudi Arabia: Saudi Arabian Deputy Ministry for Mineral Resources Open-File Report BRGM-OF-03-17, 57 p., scale 1:100,000.

Coleman, R. G.,1977, Ophiolites, (eds. Wyllie, P.J., Engelhardt, W., and Hahn, T.), Springer-Verlag, New York, 229 p.

Delfour, J., 1977, Geology of the Nuqrah quadrangle, sheet 25E, Kingdom of Saudi Arabia: Saudi Arabian Deputy Ministry for Mineral Resources Geologic Map GM-28, 32 p., scale 1:250,000.

_____ 1981, Geology of the Al Hissu quadrangle, sheet 24E, Kingdom of Saudi Arabia: Saudi Arabian Deputy Ministry for Mineral Resources Geologic Map GM-58A, 47 p., scale 1:250,000.

Duhamel, M., and Petot, J., 1972, Geology and mineral exploration of the Al Hissu quadrangle: Bureau de Recherches Geologiques et Minieres Technical Record 72-JED-7, 57 p.

Dick, H. J. B., and Bullen, T., 1984, Chromian spinel as a petrogenetic indicator in abyssal and alpine-type peridotites and spatially associated lavas: Contributions to Mineralogy and Petrology, v. 86, p. 54-76.

Johnson, P. R., 1983, A preliminary lithofacies map of the Saudi Arabian Shield: Saudi Arabian Deputy Ministry for Mineral Resources Technical Record RF-TR-03-2, 72 p., scale 1:1,000,000.

Irvine, T. N., and Baragar, W. R. A., 1971, A guide to the chemical classification of the common volcanic rocks: Canadian Journal of Earth Science, v. 8, no. 5, p. 523-548.

Leitch, E. C., 1984, Island-arc elements and arc-related ophiolites: Tectonophysics, v. 106, p. 177-203.

Lipman, P. W., Normark, W. R., Moore, J. G., Wilson, J. B., and Gutmacher, C. E., 1988, The giant submarine Alika debris slide, Mauna Loa, Hawaii, Journal of Geophysical Research, v. 93, no. B5, p. 4279-4300.

Marsten, R. J., Groves, D. I., Hudson, D. R., and Ross, J. R., 1981, Nickel-sulfide deposits in western Australia: A review: Economic Geology, v. 76, p. 1330-1363.

Naldrett, A. J., 1981, Nickel-sulfide deposits: classification, composition, and genesis: Economic Geology, v.75, p. 628-685.

Pearce, J. A., 1979, Geochemical evidence for the genesis and eruptive setting of lavas from Tethyan ophiolites in Panayiotou, A. (ed.), Ophiolites, International Ophiolite Symposium, Cyprus, 1979, p. 261-272.

Pearce, J. A., and Cann, J. R., 1973, Tectonic setting of basic volcanic rocks determined using trace-element analyses: Earth and Planetary Science Letters, v. 19, p. 290-300.

Pearce, T.H., Gorman, B.E., and Birkett, T.C., 1977, The relationship between major element chemistry and tectonic environment of basic and intermediate volcanic rocks: Earth and Planetary Science Letters, v. 36, p. 121-132.

Quick, J. E., and Bosch, P. S., 1989, Tectonic history of the Nabitah Fault Zone, Saudi Arabia: Saudi Arabian Directorate General of Mineral Resources Technical Record USGS-TR-08-2, 89 p. USGS Open-File Report (in press)

Quick, J. E., and Helaby, A. M., 1988, XAP, a spectral deconvolution program: Saudi Arabian Directorate General of Mineral Resources Technical Record USGS-TR-08-3, 33p.USGS Open-File Report 89-338.

Schmidt, D.L., Hadley, D.G., and Stoeser, D.B., 1978, Late Proterozoic crustal history of the Arabian Shield, southern Najd Province, Kingdom of Saudi Arabia, in Tahoun, S.A. (ed.), Evolution and mineralization of the Arabian-Nubian Shield, King Abdulaziz University Institute of Applied Geology Bulletin, v. 3, Pergammon, Oxford, p. 41-57.

Shervais, John, W. and Kimbrough, David, L., 1985, Geochemical evidence for the tectonic setting of the Coast Range ophiolite: A composite island arc-oceanic crust terrane in western California, Geology, v. 13, p. 35-38.

Smith, E. A., and Johnson, P. R., 1986, Selected mineral occurrences of the Arabian Shield, showing their relationship to major Precambrian tectonostratigraphic entities: Saudi Arabian Deputy Ministry for Mineral sources Technical Record RF-TR-06-1, 143 p., scale 1:1,000,000.

Snoke, A.W., Quick, J.E., and Bowman, H.R., 1981, Bear Mountains Igneous Complex, Klamath Mountains, California: An ultrabasic to silicic calc-alkaline suite: Journal of Petrology, v. 22, no. 4, p. 501-552.

Stern, R.J. and Bibee, L.D., 1984, Esmeralda Bank: Geochemistry of an active submarine volcano in the Mariana Island Arc: Contributions to Mineralogy and Petrology, v. 86, p. 159-169.

APPENDIX A.--Description of analysed samples.

SAMPLE	MAP UNIT	DESCRIPTION
240 045	t	metatuff aureole, gabbro dke
240 046	t	metatuff aureole, gabbro dke
240 047	"t"	gb2 dike cutting t
240 048	"t"	tuff xnolth (gb2) dke cuts t
240 078	dg	massive diabase
240 079	dg	massive diabase
240 130	qdb	very fine-grd diorite
240 133	"dp"	diorite (qdp) dke cuts dp
240 135	gb	fine-grained gabbro
240 136	dg	very fine-grained diabase
240 137	dg	fine-grained diabase
240 138	"dp"	fine-gained diabase dke
240 139	dp	fine-grnd diabase prphyry
240 140	"dp"	microdiorite dke cuts dp
240 141	"dp"	granophyre dike cuts dp
240 142	mgd	fine-grained grndiorte dke
240 143	mgd	grndiorte host, sample 240 142
240 144	afg	granophyre
240 145	d	diabase
240 146	f	fine-grained quartz porphyry
240 147	qdb	fine-grnd hrnbld porphyry
240 174	bb	clast in basaltic flow breccia
240 220	l	Na-rhyolt clast in lahar
240 221		fine-grnd plagiogrnt dke
240 222	mqd	fine-grnd diorite porphyry
240 225	l	Na-rhyolt clast in lahar
240 226	wt	fissile, welded tuff
240 227	"wt"	diort dke cuts wlded tuff(wt)
240 228	wt	welded tuff
240 229	wt	wlded tuff; epidte in mtrx
240 230	wt	wlded tuff; epidte in mtrx
240 231	wt	welded tuff
240 232	wt	wlded tuff 50m frm flt/qtz veins
240 233	t	dk-gry tuff 20m frm flt/qtz veins
240 235	wt	wlded tuff 10m frm grnophr dke
240 236	wt	welded tuff
240 237	wt	wlded tuff 2m frm grnophr sill
240 238	wt	wlded tuff; epidote-rich
240 239	wt	wlded tuff; epidote-rich
240 240	wt	wlded tuff; quartz phyric
240 241	t	dk-gry tuff; plag phyrc, epidt rich
240 242	t	dk gry tuff; plag phyrc
240 243	"t"	grnt dke cuts tuff; defrmd by flt
240 244	b	highly foliated basalt
240 245	b	vessic bslt; sparse vessicles
240 246	b	vsic bslt; undfmd lens in foltd bslt
240 249	b	foltd vessic basalt; sparse vessic
240 252	b	vess basalt; sparse vessicles
240 253A	b	weakly vesic bslt w/CO3 veins
240 253B	bl	vesic andrst, CO3 veins
240 254	bl	plag phyrc andste, CO3 veins
240 255	bl	plag phyrc bslt, lcly brecctd
240 256	bl	brcctd vesc bslt, CO3 veins
240 257	bl	aphanitic massive basalt
240 258	bl	brcctd vesic bslt, CO3 veins
240 259	bl	brectd, wkly vesc bslt CO3 veins
240 260	bl	lg blk in bslt brecca, CO3 matrx
240 261	bl	lg blk in bslt brecca; CO3 matrx
240 262	bb	bsltic tuff; abndnt CO3 matrx
240 263	bb	bsltic tuff; abndnt CO3 matrx
240 264	d	diabse, frctd, 30m frm qtz dio dke
240 265	d	diabase w/abndnt CO3 veins
240 266	d	diabase
240 267	d	diabase
240 268	d	diabase
240 269	b	wkly vessicular basalt
240 270	b	crse-grnd, loclly vesic basalt
240 272	b	highly fractured pillow basalt
240 273	b	bslt, CO3 vns 4m frm gbro sill
240 274	b	pillow bslt, abndant CO3 veins
240 275	b	coarse-grnd massive basalt
240 276	b	vessicular pillow basalt
240 277	b	brecctd bslt w/abndnt CO3 matrx
240 278	b	brectd vesic pillow basalt
240 322	t	dark-gray welded tuff
240 323	t	medium-gray welded tuff
240 324	t	medium gray tuff
240 325	t	dark-gray welded tuff
240 326	t	light-gray welded tuff
240 327	t	dark-gray welded tuff
240 328	gb2	crse-grnd pyroxene gabbro
240 329	b	bsalt, abundant CO3 in vugs
240 330	b	baslt, abundant CO3 in vugs
240 331	b	basalt w/minor sulfides
240 333	b	basalt
240 334	b	basalt
240 335	b	lt-grn hydrthrmly altd(?) bslt
240 337	b	lt-grn hydrthrmly altd(?) bslt
240 339	b	lt-grn hydrthrmly altd(?) bslt
240 346	b	basaltic breccia
240 347	b	basalt
240 348	b	basalt
240 350	b	basalt
240 354	dp	plag-phyric diabase, brecctd
240 355	dp	plag-phyric diabase; brecctd
240 356	dp	plag-phyric diabase; brecctd
240 357	qd	fine-med-grnd diorite
240 358	qd	fine-med-grnd diorite
240 359	gb	fine-grained pyroxene gabbro
240 360	dp	plagioclase-phyric diabase
240 361	dp	plagioclase-phyric diabase
240 362	qd	fine-grained diorite
240 363	qd	fine-grained diorite
240 364	gb	medium-grained gabbro
240 366	qdz	med-grnd hornbld qtz dio
240 367	qdz	grnodiorte dke cuts sample 366
240 369	"c"	grnodiort dke cuts clnopyroxnt
240 370	"sk"	grano dke cuts Kaffan; cut by flt
240 371	"sk"	grano dke cuts Kaffan; cuts flt
240 372	qdz	grano dke cuts Zaynah qtz diorite
240 373	qdz	grano dke cuts Zaynah qtz diorite
240 374	qdz	Zaynah qtz dio (host to 372, 373)
240 375	d	diorite
240 376	d	diorite
240 377	d	diorite
240 378	d	diorite
240 379	"d"	qtz dio dke (qdb) cuts diorite
240 380	d	diorite
240 381	qdb	medium-grnd hbl qtz diorite
240 382	dp	plagioclase-phyric felsite
240 383	dp	plagioclase-phyric diabase
240 384	dg	microgab cut by epidote/qtz veins

APPENDIX A--Description of analysed samples--(continued)

SAMPLE	MAP UNIT	DESCRIPTION
240 385	dg	microgab cut by epidote/qtz veins
240 386	dp	mafic hornfels
240 387	dg	microgab cut by epidote/qtz veins
240 388	gb	fine-grained gabbro
240 389	dg	microgab cut by epidote/qtz veins
240 392	dg	diabase
240 393	dg	microgabbro
240 395	gb	gabbro
240 396	gb	gabbro
240 397	gb	pyroxene-phyric gabbro
240 398	mgd	lt-grn plag-phyric micrograno
240 399	mgd	lt-grn plag-phyric micrograno
240 400	mqd	plagio-phyric qtz microdiorite
240 401	gb	fine-grained gabbro
240 402	gb	medium-grained gabbro
240 403	gb	1-m-thick, clinpyrox-rich gbro dke
240 404	gb	fine-grained gabbro
240 405	gb	medium-grained gabbro

APPENDIX B.—Abundances of major, minor, and trace elements, and normative minerals in representative rocks of the Bi'r Nifazi quadrangle.

Sample	240 045	240 046	240 047	240 048	240 078	240 079	240 130
				Major and Minor Elements (Percent)			
NA2O	3.39	1.98	0.58	0.70	3.25	3.42	2.52
MGO	6.27	5.44	5.94	5.42	5.85	4.68	3.82
AL2O3	14.05	12.31	16.26	22.09	14.64	15.78	15.65
SIO2	60.25	55.76	41.22	40.92	53.69	54.74	59.71
K2O	0.23	0.35	0.11	0.18	0.17	0.38	2.56
CAO	2.93	11.65	19.68	20.03	7.54	8.20	5.64
TIO2	1.31	1.42	0.87	0.79	1.49	0.60	0.81
CR2O3	0.01	0.01	0.05	0.05	0.04	0.01	0.01
MNO	0.16	0.16	0.24	0.12	0.23	0.21	0.17
FEO	10.60	10.00	13.76	10.74	11.96	12.06	8.48
P2O5	0.23	0.30	0.27	0.19	0.06	0.07	0.13
SUM	99.42	99.38	98.98	101.24	98.91	100.16	99.51
MG#	0.583	0.568	0.487	0.532	0.536	0.457	0.506
				Trace Elements (Parts per Million)			
CU	59	68	---	16	25	79	17
ZN	103	142	117	124	96	84	113
RB	8	19	7	---	7	16	74
SR	101	147	819	733	213	263	164
Y	40	35	21	12	36	7	26
ZR	110	71	28	31	98	37	146
NB	7	---	---	---	---	---	5
LA	10	27	19	---	8	---	9
ND	29	---	---	35	43	17	20
BA	119	176	46	43	192	155	284
CE	15	14	8	8	11	7	33
				CIPW Normative Minerals (Percent)			
Q	18.151	11.551	0.000	0.000	4.545	3.669	13.069
C	3.496	0.000	0.000	0.000	0.000	0.000	0.000
OR	1.345	2.054	0.000	0.000	0.995	2.257	15.175
AB	28.783	16.798	0.000	0.000	27.772	28.851	21.410
AN	13.045	23.814	41.794	55.833	25.104	26.498	23.943
LC	0.000	0.000	0.502	0.805	0.000	0.000	0.000
NE	0.000	0.000	2.694	3.184	0.000	0.000	0.000
DI	0.000	26.743	27.213	9.798	10.197	11.415	2.735
WO	0.000	0.000	0.000	0.000	0.000	0.000	0.000
HY	30.399	13.994	0.000	0.000	26.408	24.059	20.428
OL	0.000	0.000	16.262	17.645	0.000	0.000	0.000
CS	0.000	0.000	6.923	9.045	0.000	0.000	0.000
MT	1.715	1.620	2.237	1.707	1.946	1.938	1.371
CM	0.018	0.016	0.075	0.071	0.055	0.018	0.019
IL	2.505	2.717	1.662	1.483	2.851	1.128	1.546
AP	0.556	0.711	0.655	0.441	0.134	0.174	0.313

APPENDIX B.—Abundances of major, minor, and trace elements, and normative minerals in representative rocks of the Bi'r Nifazi quadrangle--(continued).

Sample	240 133	240 135	240 136	240 137	240 138	240 139	240 140	240 141
				Major and Minor Elements (Percent)				
NA2O	3.37	3.57	2.27	2.09	2.24	3.37	5.11	3.32
MGO	5.35	4.37	3.53	5.12	7.85	5.08	2.16	0.00
AL2O3	19.85	15.43	14.98	16.81	16.23	17.31	17.70	12.47
SIO2	48.58	57.96	57.10	53.35	49.87	51.40	61.98	74.29
K2O	1.43	1.29	0.39	0.15	0.87	0.58	0.78	3.53
CAO	9.64	6.69	11.34	7.94	11.73	11.20	5.89	0.58
TIO2	0.69	0.61	0.52	0.66	1.05	1.07	0.43	0.24
CR2O3	0.02	0.00	0.03	0.04	0.00	0.01	0.00	0.00
MNO	0.17	0.14	0.12	0.23	0.17	0.18	0.02	0.10
FEO	9.31	10.70	8.61	12.55	10.72	9.66	5.45	2.28
P2O5	0.12	0.12	0.09	0.02	0.08	0.11	0.20	0.00
SUM	98.52	100.88	98.98	98.96	100.82	99.96	99.72	96.81
MG#	0.561	0.473	0.475	0.470	0.627	0.549	0.474	0.000
				Trace Elements (Parts per Million)				
CU	85	111	14	300	34	96	18	12
ZN	110	78	129	127	87	69	43	101
RB	28	37	11	9	25	21	26	71
SR	564	389	190	227	323	468	508	42
Y	16	28	20	18	24	28	20	70
ZR	37	53	57	44	57	67	84	311
NB	5	---	4	---	---	6	5	8
LA	4	17	31	1	1	1	23	27
ND	11	25	---	---	7	18	13	47
BA	621	625	497	55	292	303	421	1298
CE	15	27	24	24	3	20	21	58
				CIPW Normative Minerals (Percent)				
Q	0.000	6.599	13.031	8.213	0.000	0.000	11.508	39.984
C	0.000	0.000	0.000	0.000	0.000	0.000	0.000	2.208
OR	8.550	7.565	2.350	0.892	5.111	3.434	4.596	21.551
AB	23.205	29.894	19.388	17.823	18.816	28.497	43.371	28.983
AN	35.289	22.051	29.795	36.389	31.328	30.352	23.088	2.964
LC	0.000	0.000	0.000	0.000	0.000	0.000	0.000	0.000
NE	3.101	0.000	0.000	0.000	0.000	0.000	0.000	0.000
DI	10.276	8.424	22.124	2.713	21.152	20.305	4.090	0.000
WO	0.000	0.000	0.000	0.000	0.000	0.000	0.000	0.000
HY	0.000	22.347	10.664	30.563	7.596	6.205	11.178	3.457
OL	16.428	0.000	0.000	0.000	12.119	7.350	0.000	0.000
CS	0.000	0.000	0.000	0.000	0.000	0.000	0.000	0.000
MT	1.521	1.708	1.400	2.041	1.711	1.556	0.880	0.379
CM	0.025	0.000	0.045	0.063	0.000	0.020	0.000	0.000
IL	1.335	1.148	1.002	1.264	1.978	2.037	0.827	0.475
AP	0.278	0.272	0.205	0.043	0.196	0.252	0.472	0.000

APPENDIX B.--Abundances of major, minor, and trace elements, and normative minerals in representative rocks of the Bi'r Nifazi quadrangle--(continued).

Sample	240 142	240 143	240 144	240 145	240 146	240 147	240 174
				Major and Minor Elements (Percent)			
NA2O	3.78	4.15	4.10	2.79	3.71	4.20	5.69
MGO	1.31	1.56	0.00	7.30	4.54	1.65	1.27
AL2O3	15.58	15.06	12.38	13.27	15.23	17.50	15.08
SIO2	66.04	62.56	74.83	55.28	62.66	63.82	60.41
K2O	2.04	1.86	3.16	0.20	0.29	2.03	0.23
CAO	4.14	4.40	1.03	9.72	6.44	4.59	8.55
TIO2	0.64	1.25	0.37	0.76	0.29	0.43	1.18
CR2O3	0.04	0.02	0.00	0.02	0.03	0.01	0.02
MNO	0.13	0.20	0.03	0.29	0.11	0.06	0.16
FEO	6.28	7.87	2.98	9.53	5.34	4.56	4.60
P2O5	0.21	0.44	0.00	0.00	0.10	0.17	0.76
SUM	100.20	99.38	98.88	99.16	98.73	99.03	97.94
MG#	0.323	0.326	0.000	0.628	0.649	0.454	0.429
				Trace Elements (Parts per Million)			
CU	24	23	22	66	11	40	6
ZN	94	124	132	98	81	47	104
RB	40	45	55	13	11	69	10
SR	374	450	88	86	203	575	370
Y	22	45	49	17	11	17	36
ZR	91	158	258	57	96	100	148
NB	9	4	10	6	6	---	7
LA	27	22	38	---	9	14	23
ND	25	22	55	18	16	33	27
BA	762	664	984	141	73	666	294
CE	35	50	69	5	---	18	42
				CIPW Normative Minerals (Percent)			
Q	21.883	16.480	35.206	5.603	17.793	16.994	10.952
C	0.134	0.000	0.354	0.000	0.000	0.454	0.000
OR	12.037	11.028	18.895	1.173	1.728	12.133	1.367
AB	31.885	35.322	35.042	23.800	31.813	35.842	49.116
AN	19.097	17.069	5.154	23.271	24.321	21.873	15.261
LC	0.000	0.000	0.000	0.000	0.000	0.000	0.000
NE	0.000	0.000	0.000	0.000	0.000	0.000	0.000
DI	0.000	1.725	0.000	20.753	6.041	0.000	17.526
WO	0.000	0.000	0.000	0.000	0.000	0.000	0.917
HY	12.187	13.657	4.160	22.376	16.611	10.725	0.000
OL	0.000	0.000	0.000	0.000	0.000	0.000	0.000
CS	0.000	0.000	0.000	0.000	0.000	0.000	0.000
MT	1.010	1.276	0.486	1.548	0.871	0.741	0.756
CM	0.054	0.035	0.000	0.030	0.041	0.017	0.037
IL	1.219	2.392	0.704	1.449	0.556	0.829	2.282
AP	0.507	1.042	0.000	0.000	0.231	0.401	1.826

APPENDIX B.--Abundances of major, minor, and trace elements, and normative minerals in representative rocks of the Bi'r Nifazi quadrangle--(continued).

Sample	240 220	240 221	240 222	240 225
			Major and Minor Elements (Percent)	
NA2O	4.10	4.48	3.80	4.46
MGO	1.05	0.04	1.82	1.11
AL2O3	12.96	10.84	16.85	14.15
SIO2	73.28	76.76	62.42	69.28
K2O	0.37	0.13	3.33	0.50
CAO	3.74	4.55	4.68	5.71
TIO2	0.28	0.38	0.78	0.48
CR2O3	0.00	0.03	0.03	0.02
MNO	0.07	0.08	0.07	0.13
FEO	2.86	1.44	5.60	2.42
P2O5	0.07	0.21	0.30	0.24
SUM	98.77	98.93	99.69	98.49
MG#	0.453	0.073	0.441	0.531
			Trace Elements (Parts per Million)	
CU	---	---	57	32
ZN	61	42	90	36
RB	14	8	62	15
SR	402	205	485	490
Y	13	34	28	13
ZR	124	141	154	128
NB	9	6	8	---
LA	34	13	36	28
ND	13	29	44	25
BA	630	312	1638	425
CE	54	26	34	46
			CIPW Normative Minerals (Percent)	
Q	37.712	43.271	12.757	29.288
C	0.000	0.000	0.000	0.000
OR	2.200	0.779	19.748	2.985
AB	35.097	38.292	32.202	38.304
AN	16.087	9.176	19.132	17.380
LC	0.000	0.000	0.000	0.000
NE	0.000	0.000	0.000	0.000
DI	1.862	3.557	1.855	8.124
WO	0.000	3.424	0.000	0.000
HY	5.878	0.000	11.168	2.007
OL	0.000	0.000	0.000	0.000
CS	0.000	0.000	0.000	0.000
MT	0.466	0.235	0.904	0.396
CM	0.000	0.052	0.051	0.026
IL	0.532	0.721	1.494	0.930
AP	0.171	0.507	0.705	0.574

APPENDIX B.--Abundances of major, minor, and trace elements, and normative minerals in representative rocks of the Bi'r Nifazi quadrangle--(continued).

Sample	240 226	240 227	240 228	240 229	240 230	240 231	240 232	240 233
				Major and Minor Elements (Percent)				
NA2O	1.99	4.26	3.83	3.16	4.45	4.43	4.68	5.07
MGO	1.72	2.64	1.38	1.34	0.71	1.26	0.07	2.88
AL2O3	9.84	16.67	13.62	11.39	12.58	14.21	12.65	14.19
SIO2	85.27	58.89	68.53	69.44	67.35	70.47	75.70	61.76
K2O	0.96	1.81	0.64	1.10	0.60	1.79	0.77	0.58
CAO	0.38	5.68	6.72	7.44	10.03	2.17	3.17	5.96
TIO2	0.05	1.15	0.58	0.47	0.37	0.57	0.14	0.81
CR2O3	0.00	0.01	0.04	0.05	0.02	0.00	0.01	0.01
MNO	0.04	0.14	0.21	0.14	0.17	0.13	0.08	0.13
FEO	1.40	8.12	4.89	4.26	3.55	3.55	2.26	7.27
P2O5	0.00	0.24	0.06	0.17	0.14	0.22	0.04	0.26
SUM	101.64	99.63	100.51	98.96	99.96	98.79	99.59	98.94
MG#	0.721	0.440	0.391	0.418	0.307	0.459	0.067	0.479
				Trace Elements (Parts per Million)				
CU	28	---	3	80	---	---	---	78
ZN	58	147	76	67	29	56	97	111
RB	27	45	15	33	12	28	21	16
SR	93	439	303	215	227	117	165	492
Y	41	38	38	40	47	31	34	30
ZR	170	148	204	144	180	201	205	121
NB	7	8	10	7	8	9	6	7
LA	12	17	27	27	14	46	39	27
ND	15	39	18	36	31	42	44	9
BA	919	892	330	595	309	843	372	676
CE	18	34	55	29	50	56	63	59
				CIPW Normative Minerals (Percent)				
Q	64.567	7.971	27.355	31.699	22.485	30.085	38.233	12.109
C	4.746	0.000	0.000	0.000	0.000	1.580	0.000	0.000
OR	5.602	10.707	3.777	6.554	3.539	10.704	4.551	3.460
AB	16.582	36.136	32.226	27.037	37.659	37.949	39.788	43.358
AN	1.853	21.105	17.983	13.782	12.573	9.445	11.276	14.366
LC	0.000	0.000	0.000	0.000	0.000	0.000	0.000	0.000
NE	0.000	0.000	0.000	0.000	0.000	0.000	0.000	0.000
DI	0.000	4.700	12.533	18.836	13.620	0.000	3.736	11.537
WO	0.000	0.000	0.000	0.033	8.489	0.000	0.000	0.000
HY	6.337	15.303	4.053	0.000	0.000	8.053	1.665	11.796
OL	0.000	0.000	0.000	0.000	0.000	0.000	0.000	0.000
CS	0.000	0.000	0.000	0.000	0.000	0.000	0.000	0.000
MT	0.222	1.313	0.784	0.693	0.571	0.578	0.365	1.183
CM	0.000	0.020	0.055	0.073	0.026	0.000	0.021	0.018
IL	0.092	2.183	1.095	0.900	0.708	1.090	0.264	1.562
AP	0.000	0.577	0.145	0.403	0.339	0.529	0.106	0.625

APPENDIX B.--Abundances of major, minor, and trace elements, and normative minerals in representative rocks of the Bi'r Nifazi quadrangle--(continued).

Sample	240 235	240 236	240 237	240 238	240 239	240 240	240 241	240 242
				Major and Minor Elements (Percent)				
NA2O	4.65	4.38	3.50	3.62	3.64	2.00	5.23	4.78
MGO	6.62	1.42	1.39	1.35	0.98	0.81	1.54	2.38
AL2O3	18.11	13.87	13.37	14.16	13.06	12.94	16.93	17.61
SIO2	51.78	70.73	71.36	71.19	77.64	72.03	62.02	61.32
K2O	0.24	0.88	1.74	1.05	0.61	3.62	1.14	1.20
CAO	7.74	2.30	4.86	3.39	2.25	5.42	6.12	5.21
TIO2	0.84	0.67	0.24	0.60	0.07	0.19	0.81	0.72
CR2O3	0.05	0.03	0.02	0.02	0.02	0.01	0.03	0.04
MNO	0.13	0.12	0.15	0.09	0.12	0.11	0.12	0.06
FEO	10.06	4.32	3.95	3.75	2.73	2.33	5.58	6.13
P2O5	0.23	0.26	0.04	0.24	0.12	0.03	0.08	0.19
SUM	100.44	98.98	100.63	99.44	101.23	99.51	99.59	99.63
MG#	0.599	0.443	0.431	0.467	0.424	0.430	0.400	0.479
				Trace Elements (Parts per Million)				
CU	105	---	63	24	---	41	55	39
ZN	112	107	108	72	96	60	79	70
RB	13	23	35	26	21	74	23	29
SR	736	268	165	199	119	185	550	531
Y	16	33	13	40	37	7	22	24
ZR	84	167	104	186	214	96	119	132
NB	6	8	7	11	9	7	6	9
LA	30	35	43	53	53	35	20	23
ND	---	19	12	29	38	24	35	25
BA	150	1826	624	1272	190	1058	646	617
CE	45	51	31	70	70	46	44	37
				CIPW Normative Minerals (Percent)				
Q	0.000	33.230	30.779	35.402	45.621	34.754	10.907	11.310
C	0.000	2.179	0.000	1.470	2.570	0.000	0.000	0.000
OR	1.409	5.277	10.241	6.224	3.586	21.486	6.788	7.092
AB	39.151	37.442	29.412	30.798	30.395	16.992	44.393	40.528
AN	27.672	9.763	15.516	15.368	10.263	15.731	19.412	23.150
LC	0.000	0.000	0.000	0.000	0.000	0.000	0.000	0.000
NE	0.000	0.000	0.000	0.000	0.000	0.000	0.000	0.000
DI	7.456	0.000	6.898	0.000	0.000	9.328	8.921	1.283
WO	0.000	0.000	0.000	0.000	0.000	0.000	0.000	0.000
HY	2.213	9.463	5.946	8.414	6.706	0.870	6.904	13.779
OL	18.322	0.000	0.000	0.000	0.000	0.000	0.000	0.000
CS	0.000	0.000	0.000	0.000	0.000	0.000	0.000	0.000
MT	1.612	0.703	0.632	0.607	0.434	0.378	0.901	0.990
CM	0.068	0.047	0.036	0.029	0.024	0.019	0.052	0.053
IL	1.579	1.280	0.460	1.139	0.129	0.368	1.544	1.380
AP	0.531	0.631	0.084	0.561	0.277	0.077	0.184	0.445

APPENDIX B.--Abundances of major, minor, and trace elements, and normative minerals in representative rocks of the Bi'r Nifazi quadrangle--(continued).

Sample	240 243	240 244	240 245	240 246	240 249	240 252	240 253A	240 253B
				Major and Minor Elements (Percent)				
NA2O	1.76	3.24	1.30	1.90	1.72	3.75	4.59	3.71
MGO	0.85	4.16	3.30	4.55	4.86	4.36	2.80	2.61
AL2O3	11.96	16.69	13.62	16.92	16.98	16.68	16.88	17.25
SIO2	76.46	48.60	48.41	51.47	53.46	53.43	46.39	62.08
K2O	2.50	0.08	0.03	0.27	0.03	0.22	0.10	0.56
CAO	3.47	13.69	15.71	13.69	12.08	11.74	16.86	7.22
TIO2	0.26	0.62	3.03	1.58	0.77	0.69	1.51	0.72
CR2O3	0.02	0.04	0.03	0.03	0.00	0.02	0.05	0.05
MNO	0.10	0.23	0.23	0.27	0.17	0.04	0.20	0.06
FEO	2.32	10.52	12.50	9.19	9.01	8.59	9.88	6.20
P2O5	0.00	0.14	0.59	0.05	0.12	0.14	0.13	0.13
SUM	99.70	98.00	98.74	99.92	99.21	99.65	99.38	100.60
MG#	0.452	0.463	0.420	0.550	0.548	0.536	0.408	0.499
				Trace Elements (Parts per Million)				
CU	---	53	31	33	163	136	119	94
ZN	36	92	169	105	96	110	90	83
RB	74	10	---	10	11	---	8	11
SR	255	450	361	392	444	690	257	1234
Y	15	14	61	26	17	15	23	22
ZR	166	62	199	92	69	75	89	134
NB	7	6	8	6	---	8	6	9
LA	56	7	11	14	14	21	15	15
ND	24	32	29	21	11	12	15	26
BA	1114	63	40	101	114	23	43	398
CE	71	24	57	18	18	16	15	17
				CIPW Normative Minerals (Percent)				
Q	46.568	0.000	6.380	4.506	9.086	0.247	0.000	16.708
C	0.045	0.000	0.000	0.000	0.000	0.000	0.000	0.000
OR	14.811	0.478	0.193	1.605	0.179	1.311	0.574	3.300
AB	14.907	22.895	11.096	16.035	14.678	31.769	7.892	31.170
AN	17.278	31.350	31.592	36.862	38.787	28.129	25.324	28.559
LC	0.000	0.000	0.000	0.000	0.000	0.000	0.000	0.000
NE	0.000	2.726	0.000	0.000	0.000	0.000	16.855	0.000
DI	0.000	31.006	36.526	25.457	17.215	24.392	40.167	5.142
WO	0.000	0.000	0.000	0.000	0.000	0.000	4.337	0.000
HY	5.493	0.000	4.913	10.904	16.835	11.110	0.000	12.391
OL	0.000	8.219	0.000	0.000	0.000	0.000	0.000	0.000
CS	0.000	0.000	0.000	0.000	0.000	0.000	0.000	0.000
MT	0.375	1.727	2.037	1.480	1.461	1.387	1.601	0.993
CM	0.031	0.067	0.048	0.046	0.000	0.027	0.067	0.068
IL	0.494	1.209	5.824	2.992	1.473	1.307	2.879	1.366
AP	0.000	0.333	1.425	0.120	0.294	0.328	0.313	0.311

APPENDIX B.--Abundances of major, minor, and trace elements, and normative minerals in representative rocks of the Bi'r Nifazi quadrangle--(continued).

Sample	240 254	240 255	240 256	240 257	240 258	240 259	240 260	240 26
				Major and Minor Elements (Percent)				
NA2O	4.81	3.25	4.34	3.32	5.24	3.80	4.01	3.56
MGO	2.32	5.29	3.84	4.73	4.48	5.45	3.93	4.34
AL2O3	17.27	19.89	19.22	18.72	17.18	17.66	18.16	18.26
SIO2	61.57	51.35	52.77	52.35	51.49	52.46	53.49	50.44
K2O	0.27	0.66	0.92	0.73	0.12	0.51	0.97	0.59
CAO	5.52	10.60	9.96	9.70	12.01	10.22	8.82	12.10
TIO2	0.86	1.31	1.06	1.03	1.28	1.29	1.34	1.36
CR2O3	0.02	0.01	0.02	0.02	0.06	0.03	0.04	0.06
MNO	0.10	0.13	0.21	0.19	0.09	0.09	0.06	0.13
FEO	6.06	7.84	7.66	8.43	9.13	8.34	8.57	9.20
P2O5	0.10	0.19	0.17	0.21	0.12	0.16	0.09	0.22
SUM	98.89	100.52	100.17	99.42	101.20	100.01	99.46	100.25
MG#	0.481	0.627	0.543	0.568	0.545	0.618	0.534	0.536
				Trace Elements (Parts per Million)				
CU	32	64	75	42	41	46	28	31
ZN	109	132	46	79	101	81	80	73
RB	12	21	20	19	14	19	15	16
SR	888	526	545	514	464	872	533	795
Y	22	20	23	22	28	23	29	30
ZR	149	115	141	117	112	116	116	119
NB	8	8	8	7	8	8	11	9
LA	20	1	12	13	18	13	9	14
ND	22	11	11	54	20	33	20	16
BA	171	132	234	269	86	173	251	224
CE	25	41	21	40	17	37	27	19
				CIPW Normative Minerals (Percent)				
Q	14.402	0.000	0.000	0.371	0.000	0.000	0.000	0.000
C	0.000	0.000	0.000	0.000	0.000	0.000	0.000	0.000
OR	1.596	3.898	5.443	4.310	0.686	2.999	5.734	3.471
AB	41.140	27.314	36.265	28.262	28.475	32.120	34.045	27.828
AN	24.995	37.491	30.158	34.188	22.716	29.594	28.846	32.004
LC	0.000	0.000	0.000	0.000	0.000	0.000	0.000	0.000
NE	0.000	0.000	0.191	0.000	8.274	0.000	0.000	1.181
DI	1.692	11.121	14.927	10.584	29.328	16.450	12.040	21.932
WO	0.000	0.000	0.000	0.000	0.000	0.000	0.000	0.000
HY	13.273	10.815	0.000	18.451	0.000	9.529	15.118	0.000
OL	0.000	5.183	9.347	0.000	6.297	5.110	0.015	8.957
CS	0.000	0.000	0.000	0.000	0.000	0.000	0.000	0.000
MT	0.987	1.256	1.232	1.364	1.452	1.343	1.386	1.477
CM	0.027	0.017	0.033	0.025	0.089	0.038	0.053	0.084
IL	1.656	2.469	2.005	1.965	2.407	2.447	2.548	2.570
AP	0.238	0.446	0.411	0.494	0.283	0.380	0.220	0.509

APPENDIX B.--Abundances of major, minor, and trace elements, and normative minerals in representative rocks of the Bi'r Nifazi quadrangle--(continued).

Sample	240 262	240 263	240 264	240 265	240 266	240 267	240 268	240 269
				Major and Minor Elements (Percent)				
NA2O	2.68	2.16	2.57	3.44	3.31	3.41	1.42	5.60
MGO	3.57	2.62	3.88	4.40	6.06	4.22	4.31	3.81
AL2O3	14.45	15.58	13.12	14.45	15.18	13.76	14.26	15.06
SIO2	40.42	46.80	59.26	53.52	49.79	57.72	54.48	49.96
K2O	0.35	0.79	0.08	0.13	0.45	0.11	1.00	0.27
CAO	28.99	23.66	6.51	7.44	10.53	5.52	8.03	6.99
TIO2	1.22	1.20	1.82	1.93	1.49	1.75	2.14	3.33
CR2O3	0.02	0.01	0.00	0.04	0.00	0.03	0.03	0.05
MNO	0.21	0.11	0.17	0.20	0.19	0.18	0.21	0.25
FEO	6.64	7.26	11.43	13.63	12.10	12.04	12.58	12.70
P2O5	0.44	0.28	0.12	0.12	0.09	0.09	0.20	0.51
SUM	98.96	100.47	98.97	99.30	99.20	98.84	98.66	98.50
MG#	0.572	0.473	0.456	0.439	0.541	0.460	0.462	0.458
				Trace Elements (Parts per Million)				
CU	87	65	9	---	35	44	53	88
ZN	113	98	132	141	106	142	123	181
RB	---	19	---	10	18	13	26	14
SR	841	427	145	117	111	265	80	200
Y	17	22	36	38	32	45	47	67
ZR	96	109	117	115	82	122	124	229
NB	10	7	---	---	6	---	4	---
LA	27	7	---	---	9	2	---	6
ND	17	15	26	21	26	19	27	26
BA	207	218	64	73	83	139	183	125
CE	48	9	30	19	---	17	17	45
				CIPW Normative Minerals (Percent)				
Q	0.000	0.000	19.505	5.205	0.000	13.387	13.949	0.000
C	0.000	0.000	0.000	0.000	0.000	0.000	0.000	0.000
OR	0.000	3.730	0.476	0.766	2.649	0.662	5.958	1.627
AB	0.000	0.000	21.963	29.263	28.196	29.186	12.149	44.420
AN	26.629	30.301	24.238	23.748	25.412	22.132	29.970	15.377
LC	1.633	0.706	0.000	0.000	0.000	0.000	0.000	0.000
NE	12.393	9.865	0.000	0.000	0.000	0.000	0.000	1.939
DI	22.917	31.833	6.344	10.591	22.068	4.132	7.582	13.775
WO	0.000	19.471	0.000	0.000	0.000	0.000	0.000	0.000
HY	0.000	0.000	21.843	24.191	4.014	24.926	23.714	0.000
OL	4.733	0.000	0.000	0.000	12.623	0.000	0.000	13.127
CS	27.232	0.000	0.000	0.000	0.000	0.000	0.000	0.000
MT	1.080	1.164	1.858	2.208	1.963	1.960	2.052	2.074
CM	0.032	0.019	0.000	0.052	0.000	0.049	0.052	0.074
IL	2.331	2.274	3.495	3.693	2.857	3.353	4.116	6.403
AP	1.045	0.653	0.287	0.291	0.224	0.220	0.471	1.215

APPENDIX B.--Abundances of major, minor, and trace elements, and normative minerals in representative rocks of the Bi'r Nifazi quadrangle--(continued).

Sample	240 270	240 272	240 273	240 274	240 275	240 276	240 277	240 278
				Major and Minor Elements (Percent)				
NA2O	2.70	5.16	3.35	6.21	2.96	1.57	1.91	6.58
MGO	3.91	4.69	4.52	3.29	8.80	4.46	6.25	1.64
AL2O3	18.58	18.76	14.16	17.12	18.19	15.64	13.70	19.91
SIO2	45.70	49.97	48.18	53.22	47.70	51.89	47.87	50.89
K2O	0.43	0.36	0.23	0.11	0.30	0.84	0.20	0.48
CAO	19.63	9.26	9.91	9.96	11.19	13.27	15.84	11.22
TIO2	1.27	2.15	3.26	1.84	1.29	1.58	2.26	0.70
CR2O3	0.03	0.03	0.05	0.06	0.06	0.03	0.01	0.01
MNO	0.27	0.14	0.20	0.12	0.17	0.19	0.21	0.11
FEO	7.91	9.87	14.82	7.22	8.99	9.60	10.43	8.34
P2O5	0.15	0.21	0.17	0.18	0.06	0.07	0.10	0.16
SUM	100.57	100.59	98.87	99.34	99.70	99.14	98.80	100.04
MG#	0.544	0.559	0.450	0.562	0.703	0.535	0.613	0.307
				Trace Elements (Parts per Million)				
CU	53	120	92	60	35	33	49	88
ZN	66	118	148	104	91	71	103	87
RB	14	13	13	8	17	17	9	18
SR	259	307	309	213	246	210	254	454
Y	20	33	44	36	20	27	33	14
ZR	72	119	142	103	70	82	115	65
NB	5	---	8	---	---	5	5	---
LA	---	11	15	---	7	6	15	---
ND	---	19	16	---	2	21	14	15
BA	115	452	87	104	69	151	51	200
CE	14	16	24	15	10	15	13	13
				CIPW Normative Minerals (Percent)				
Q	0.000	0.000	0.000	0.000	0.000	5.862	0.000	0.000
C	0.000	0.000	0.000	0.000	0.000	0.000	0.000	0.000
OR	0.000	2.106	1.401	0.672	1.754	5.029	1.195	2.857
AB	0.000	32.466	28.662	41.169	21.472	13.399	16.362	26.363
AN	37.068	26.754	23.118	18.596	35.553	33.379	28.518	23.335
LC	1.979	0.000	0.000	0.000	0.000	0.000	0.000	0.000
NE	12.283	5.913	0.000	6.347	1.954	0.000	0.000	15.825
DI	40.894	14.512	21.352	24.775	15.985	27.028	41.320	26.760
WO	3.129	0.000	0.000	0.000	0.000	0.000	0.000	0.000
HY	0.000	0.000	8.890	0.000	0.000	10.522	0.346	0.000
OL	0.000	12.106	7.445	3.250	19.158	0.000	5.961	1.817
CS	0.599	0.000	0.000	0.000	0.000	0.000	0.000	0.000
MT	1.267	1.580	2.411	1.170	1.451	1.558	1.700	1.343
CM	0.042	0.038	0.075	0.090	0.084	0.042	0.021	0.015
IL	2.396	4.046	6.247	3.509	2.451	3.030	4.341	1.320
AP	0.354	0.492	0.410	0.432	0.143	0.157	0.244	0.376

APPENDIX B.--Abundances of major, minor, and trace elements, and normative minerals in representative rocks of the Bi'r Nifazi quadrangle--(continued).

Sample	240 322	240 323	240 324	240 325	240 326	240 327	240 328	240 329
				Major and Minor Elements (Percent)				
NA2O	3.43	2.68	2.86	1.79	2.48	2.51	3.21	3.25
MGO	7.26	7.32	8.32	4.12	4.85	7.05	6.43	4.86
AL2O3	15.58	14.50	14.15	14.52	16.01	17.54	17.80	14.99
SIO2	50.78	54.41	53.20	61.84	59.61	49.90	47.74	49.85
K2O	0.38	1.90	0.73	0.88	0.50	0.33	0.18	0.09
CAO	12.13	13.13	15.90	9.21	12.37	14.35	11.85	13.79
TIO2	1.19	0.42	0.33	0.74	0.56	0.67	1.47	2.35
CR2O3	0.00	0.02	0.02	0.04	0.02	0.02	0.05	0.00
MNO	0.14	0.14	0.21	0.12	0.07	0.11	0.24	0.17
FEO	9.52	5.17	4.12	5.89	3.38	7.47	11.14	9.59
P2O5	0.23	0.08	0.06	0.19	0.09	0.10	0.24	0.27
SUM	100.64	99.78	99.91	99.31	99.93	100.06	100.34	99.22
MG#	0.643	0.759	0.813	0.623	0.781	0.682	0.578	0.582
				Trace Elements (Parts per Million)				
CU	58	---	---	53	---	15	70	53
ZN	99	87	75	92	93	74	105	103
RB	19	55	19	30	22	10	13	---
SR	318	438	479	371	409	314	337	170
Y	24	11	9	26	11	15	26	42
ZR	96	145	138	117	161	58	78	123
NB	---	5	---	7	5	5	4	---
LA	6	28	21	39	9	18	8	12
ND	24	10	12	38	16	20	17	15
BA	153	653	316	370	372	96	70	64
CE	47	42	29	65	42	27	4	---
				CIPW Normative Minerals (Percent)				
Q	0.000	0.000	0.000	22.490	14.194	0.000	0.000	0.000
C	0.000	0.000	0.000	0.000	0.000	0.000	0.000	0.000
OR	2.203	11.219	4.310	5.223	2.957	1.944	1.082	0.558
AB	27.021	22.728	20.196	15.226	20.977	20.442	22.489	27.593
AN	25.785	21.970	23.615	29.169	31.095	35.554	33.464	26.205
LC	0.000	0.000	0.000	0.000	0.000	0.000	0.000	0.000
NE	0.990	0.000	2.191	0.000	0.000	0.434	2.456	0.051
DI	26.566	34.428	43.925	12.786	23.824	28.376	19.423	33.804
WO	0.000	0.000	0.000	0.000	0.000	0.000	0.000	0.000
HY	0.000	3.900	0.000	12.256	5.100	0.000	0.000	0.000
OL	13.142	3.897	4.308	0.000	0.000	10.515	15.907	5.120
CS	0.000	0.000	0.000	0.000	0.000	0.000	0.000	0.000
MT	1.522	0.835	0.664	0.955	0.545	1.202	1.787	1.555
CM	0.000	0.034	0.033	0.054	0.026	0.024	0.069	0.000
IL	2.243	0.796	0.630	1.411	1.066	1.270	2.775	4.493
AP	0.541	0.200	0.135	0.441	0.222	0.246	0.564	0.637

APPENDIX B.--Abundances of major, minor, and trace elements, and normative minerals in representative rocks of the Bi'r Nifazi quadrangle--(continued).

Sample	240 330	240 331	240 333	240 334	240 335	240 337	240 339	240 346
				Major and Minor Elements (Percent)				
NA2O	4.05	2.21	2.86	1.76	4.41	4.75	2.36	3.88
MGO	5.38	7.08	3.23	4.55	2.45	2.85	9.12	5.92
AL2O3	18.38	13.05	17.45	17.02	16.72	19.56	13.01	18.30
SIO2	48.94	44.76	46.70	49.44	46.19	50.92	46.34	48.22
K2O	0.63	0.27	0.58	0.11	0.33	0.19	0.09	0.34
CAO	14.02	17.48	16.11	13.95	18.49	13.61	19.15	11.44
TIO2	1.40	2.80	1.37	1.47	1.81	1.45	1.32	1.19
CR2O3	0.05	0.00	0.02	0.00	0.00	0.13	0.05	0.03
MNO	0.17	0.29	0.16	0.17	0.20	0.08	0.16	0.14
FEO	6.63	11.37	10.79	10.74	8.53	5.61	7.50	10.19
P2O5	0.05	0.39	0.07	0.17	0.22	0.06	0.30	0.28
SUM	99.70	99.70	99.34	99.38	99.35	99.21	99.40	99.93
MG#	0.679	0.629	0.415	0.504	0.428	0.593	0.754	0.578
				Trace Elements (Parts per Million)				
CU	58	32	57	96	81	69	80	22
ZN	82	132	77	51	88	96	98	137
RB	13	15	16	9	10	---	8	---
SR	302	219	295	421	249	253	153	866
Y	28	49	20	26	25	25	25	18
ZR	88	141	77	90	87	92	75	94
NB	5	8	4	7	6	6	4	7
LA	1	4	10	---	11	5	6	4
ND	15	20	---	14	32	---	9	5
BA	116	45	120	79	76	160	279	120
CE	9	11	3	13	15	18	8	38
				CIPW Normative Minerals (Percent)				
Q	0.000	0.000	0.000	2.378	0.000	0.000	0.000	0.000
C	0.000	0.000	0.000	0.000	0.000	0.000	0.000	0.000
OR	3.709	1.593	3.467	0.656	1.941	1.132	0.000	1.981
AB	15.545	2.403	8.432	14.986	6.583	27.570	0.000	23.095
AN	30.183	24.927	33.263	38.389	24.995	31.710	24.786	31.523
LC	0.000	0.000	0.000	0.000	0.000	0.000	0.418	0.000
NE	10.194	8.859	8.593	0.000	16.757	7.002	10.863	5.265
DI	31.957	48.733	39.365	25.078	33.475	27.499	54.364	19.311
WO	0.000	0.000	0.000	0.000	10.896	1.067	0.000	0.000
HY	0.000	0.000	0.000	13.576	0.000	0.000	0.000	0.000
OL	4.502	5.415	2.332	0.000	0.000	0.000	4.653	14.230
CS	0.000	0.000	0.000	0.000	0.000	0.000	0.411	0.000
MT	1.071	1.835	1.749	1.739	1.382	0.910	1.215	1.641
CM	0.072	0.000	0.023	0.000	0.000	0.189	0.075	0.038
IL	2.657	5.331	2.611	2.806	3.457	2.778	2.529	2.266
AP	0.114	0.927	0.172	0.403	0.527	0.148	0.704	0.666

APPENDIX B.--Abundances of major, minor, and trace elements, and normative minerals in representative rocks of the Bi'r Nifazi quadrangle--(continued).

Sample	240 347	240 348	240 350	240 354	240 355	240 356	240 357	240 358
				Major and Minor Elements (Percent)				
NA2O	3.55	4.97	4.20	2.58	1.51	2.33	3.74	3.83
MGO	3.78	4.20	3.56	4.93	6.05	5.51	3.06	3.17
AL2O3	14.19	14.46	17.79	18.32	19.22	20.66	17.99	17.91
SIO2	55.33	50.59	48.58	51.85	50.01	49.25	56.70	59.42
K2O	0.02	0.20	0.77	0.24	0.30	0.69	2.24	2.22
CAO	7.09	16.10	13.50	11.61	12.58	11.31	6.98	6.48
TIO2	2.81	1.20	1.47	0.85	0.67	0.77	0.72	0.58
CR2O3	0.05	0.02	0.04	0.04	0.00	0.02	0.00	0.00
MNO	0.12	0.23	0.13	0.05	0.14	0.13	0.23	0.16
FEO	12.64	6.79	9.81	9.95	10.10	9.60	7.88	6.75
P2O5	0.45	0.24	0.11	0.16	0.10	0.00	0.24	0.21
SUM	100.03	98.99	99.96	100.56	100.68	100.26	99.79	100.73
MG#	0.448	0.604	0.471	0.532	0.570	0.564	0.465	0.512
				Trace Elements (Parts per Million)				
CU	97	59	29	68	75	71	160	69
ZN	160	76	125	67	83	59	86	101
RB	7	8	17	11	10	16	84	74
SR	82	215	356	211	276	532	462	492
Y	60	20	30	16	11	15	23	25
ZR	200	107	89	46	38	50	89	98
NB	8	6	8	---	---	---	8	8
LA	16	22	---	5	---	28	18	29
ND	18	20	---	15	---	13	19	25
BA	32	80	304	100	164	423	565	714
CE	31	39	7	7	15	9	29	19
				CIPW Normative Minerals (Percent)				
Q	10.101	0.000	0.000	1.775	1.281	0.000	3.829	7.305
C	0.000	0.000	0.000	0.000	0.000	0.000	0.000	0.000
OR	0.146	1.175	4.545	1.416	1.746	4.085	13.272	13.016
AB	30.019	20.613	16.202	21.646	12.636	19.664	31.714	32.133
AN	22.656	16.735	27.416	37.464	44.454	43.680	25.696	24.929
LC	0.000	0.000	0.000	0.000	0.000	0.000	0.000	0.000
NE	0.000	11.816	10.441	0.000	0.000	0.000	0.000	0.000
DI	8.014	39.878	32.565	15.525	13.921	10.110	6.225	4.689
WO	0.000	5.783	0.000	0.000	0.000	0.000	0.000	0.000
HY	20.600	0.000	0.000	18.558	22.859	10.751	16.081	15.280
OL	0.000	0.000	4.157	0.000	0.000	8.689	0.000	0.000
CS	0.000	0.000	0.000	0.000	0.000	0.000	0.000	0.000
MT	2.033	1.104	1.579	1.592	1.615	1.540	1.272	1.079
CM	0.073	0.036	0.064	0.055	0.000	0.023	0.000	0.000
IL	5.327	2.294	2.790	1.597	1.260	1.459	1.366	1.093
AP	1.055	0.582	0.250	0.382	0.235	0.000	0.560	0.489

APPENDIX B.–Abundances of major, minor, and trace elements, and normative minerals in representative rocks of the Bi'r Nifazi quadrangle--(continued).

Sample	240 359	240 360	240 361	240 362	240 363	240 364	240 366	240 367
				Major and Minor Elements (Percent)				
NA2O	1.82	3.64	4.05	4.17	1.52	2.38	4.81	4.28
MGO	9.49	4.02	2.41	5.68	2.30	5.94	1.48	0.64
AL2O3	12.00	19.51	19.04	17.05	18.38	17.98	17.95	15.85
SIO2	48.58	53.01	54.48	51.52	58.91	50.64	64.90	70.09
K2O	0.23	0.58	1.79	0.22	2.68	0.34	1.85	2.05
CAO	14.67	8.99	7.74	8.78	8.29	10.94	4.22	3.41
TIO2	0.92	0.98	0.91	1.43	0.68	0.56	0.37	0.29
CR2O3	0.00	0.00	0.02	0.07	0.05	0.00	0.00	0.03
MNO	0.19	0.09	0.15	0.18	0.16	0.19	0.04	0.00
FEO	11.44	9.23	9.31	10.34	6.20	10.10	3.34	2.02
P2O5	0.00	0.05	0.27	0.28	0.17	0.11	0.32	0.04
SUM	99.34	100.11	100.17	99.72	99.34	99.18	99.27	98.69
MG#	0.651	0.504	0.372	0.569	0.461	0.562	0.510	0.441
				Trace Elements (Parts per Million)				
CU	52	69	120	80	40	72	25	25
ZN	118	116	104	93	108	111	71	69
RB	14	17	32	9	65	---	61	57
SR	245	417	461	524	259	367	435	477
Y	21	17	25	26	16	19	9	6
ZR	61	53	80	148	118	37	136	125
NB	5	7	6	7	8	---	7	5
LA	---	5	7	18	11	21	33	29
ND	17	21	---	22	19	---	9	24
BA	212	221	595	176	454	289	817	821
CE	6	5	14	32	40	5	51	31
				CIPW Normative Minerals (Percent)				
Q	0.000	0.559	0.384	0.000	16.205	0.089	17.500	28.381
C	0.000	0.000	0.000	0.000	0.000	0.000	1.142	0.496
OR	1.360	3.438	10.538	1.319	15.908	2.052	10.996	12.258
AB	15.455	30.734	34.174	35.310	12.930	20.263	40.982	36.662
AN	24.049	35.105	28.404	27.216	35.644	37.635	18.965	16.881
LC	0.000	0.000	0.000	0.000	0.000	0.000	0.000	0.000
NE	0.000	0.000	0.000	0.000	0.000	0.000	0.000	0.000
DI	40.162	7.574	6.872	12.087	3.862	13.499	0.000	0.000
WO	0.000	0.000	0.000	0.000	0.000	0.000	0.000	0.000
HY	0.409	19.129	15.754	9.679	12.676	23.498	8.418	4.310
OL	14.952	0.000	0.000	9.256	0.000	0.000	0.000	0.000
CS	0.000	0.000	0.000	0.000	0.000	0.000	0.000	0.000
MT	1.854	1.484	1.496	1.669	1.005	1.639	0.542	0.330
CM	0.000	0.000	0.024	0.108	0.072	0.000	0.000	0.047
IL	1.760	1.857	1.722	2.719	1.298	1.076	0.711	0.549
AP	0.000	0.125	0.648	0.654	0.411	0.257	0.762	0.088

APPENDIX B.–Abundances of major, minor, and trace elements, and normative minerals in representative rocks of the Bi'r Nifazi quadrangle--(continued).

Sample	240 369	240 370	240 371	240 372	240 373	240 374	240 375	240 376
				Major and Minor Elements (Percent)				
NA2O	4.73	4.39	4.27	4.41	4.48	4.15	3.36	3.11
MGO	1.36	0.81	0.67	0.51	0.59	2.05	4.17	5.65
AL2O3	16.93	17.43	16.99	15.95	15.79	18.08	13.50	14.93
SIO2	66.18	67.02	70.40	70.13	71.20	63.61	53.95	52.21
K2O	1.89	1.95	2.01	2.35	2.68	2.49	0.46	0.51
CAO	3.91	4.59	3.71	2.86	2.69	4.81	7.46	9.78
TIO2	0.41	0.37	0.25	0.31	0.20	0.53	2.08	1.40
CR2O3	0.01	0.02	0.02	0.00	0.00	0.02	0.00	0.06
MNO	0.06	0.00	0.10	0.03	0.02	0.02	0.24	0.19
FEO	3.11	2.43	2.12	2.38	2.23	3.58	13.38	10.47
P2O5	0.23	0.14	0.09	0.20	0.14	0.09	0.23	0.16
SUM	98.82	99.14	100.64	99.12	100.02	99.43	98.84	98.48
MG#	0.510	0.456	0.418	0.337	0.379	0.588	0.433	0.563
				Trace Elements (Parts per Million)				
CU	54	27	24	15	54	14	---	48
ZN	47	46	42	65	79	85	119	116
RB	56	44	53	71	74	68	16	22
SR	490	524	490	414	428	311	245	272
Y	10	5	9	7	11	6	49	33
ZR	165	113	113	171	132	142	127	81
NB	6	5	5	7	9	6	---	---
LA	22	18	35	44	30	31	14	15
ND	18	33	14	45	10	23	13	19
BA	997	797	940	1080	1064	932	252	292
CE	54	24	12	48	41	55	9	9
				CIPW Normative Minerals (Percent)				
Q	19.981	22.162	27.598	27.917	27.165	14.767	6.274	1.513
C	0.558	0.111	1.258	1.440	0.953	0.038	0.000	0.000
OR	11.312	11.603	11.800	13.981	15.823	14.819	2.754	3.078
AB	40.472	37.427	35.903	37.669	37.881	35.292	28.724	26.714
AN	18.080	22.013	17.679	12.994	12.468	23.362	20.604	25.618
LC	0.000	0.000	0.000	0.000	0.000	0.000	0.000	0.000
NE	0.000	0.000	0.000	0.000	0.000	0.000	0.000	0.000
DI	0.000	0.000	0.000	0.000	0.000	0.000	12.835	18.633
WO	0.000	0.000	0.000	0.000	0.000	0.000	0.000	0.000
HY	7.746	5.231	4.707	4.570	4.657	9.879	22.099	19.563
OL	0.000	0.000	0.000	0.000	0.000	0.000	0.000	0.000
CS	0.000	0.000	0.000	0.000	0.000	0.000	0.000	0.000
MT	0.507	0.394	0.339	0.387	0.359	0.579	2.178	1.710
CM	0.019	0.029	0.031	0.000	0.000	0.034	0.000	0.095
IL	0.787	0.699	0.470	0.584	0.376	1.015	3.993	2.694
AP	0.552	0.337	0.219	0.469	0.324	0.220	0.554	0.393

APPENDIX B.--Abundances of major, minor, and trace elements, and normative minerals in representative rocks of the Bi'r Nifazi quadrangle--(continued).

Sample	240 377	240 378	240 379	240 380	240 381	240 382	240 383	240 384
				Major and Minor Elements (Percent)				
NA2O	4.08	2.64	4.48	3.41	3.43	2.88	3.72	1.74
MGO	5.19	6.76	2.22	3.32	4.04	0.76	5.10	5.60
AL2O3	15.28	14.36	17.33	14.86	18.47	15.57	15.61	16.38
SIO2	53.09	52.33	59.35	54.13	54.24	64.76	49.98	51.54
K2O	0.24	0.26	1.62	0.50	1.40	5.52	0.49	0.14
CAO	8.82	9.44	5.11	7.62	8.25	2.58	12.21	8.29
TIO2	1.34	1.31	1.12	2.04	0.75	0.64	1.06	0.66
CR2O3	0.00	0.02	0.03	0.02	0.05	0.04	0.00	0.02
MNO	0.27	0.13	0.12	0.23	0.15	0.11	0.32	0.15
FEO	10.30	10.82	8.33	12.38	8.89	4.82	9.90	13.58
P2O5	0.03	0.11	0.38	0.38	0.44	0.21	0.35	0.17
SUM	98.63	98.18	100.09	98.90	100.13	97.88	98.75	98.27
MG#	0.542	0.597	0.390	0.399	0.507	0.272	0.539	0.474
				Trace Elements (Parts per Million)				
CU	---	36	---	---	87	100	151	304
ZN	98	110	147	140	59	72	121	121
RB	11	15	53	13	47	96	20	14
SR	108	247	390	157	602	242	541	102
Y	33	33	39	52	16	36	27	15
ZR	98	87	163	130	77	292	127	39
NB	---	---	7	6	6	13	8	7
LA	1	1	26	8	---	50	21	10
ND	24	11	29	21	22	55	28	10
BA	209	253	742	274	495	2111	257	15
CE	---	9	44	10	18	57	40	8
				CIPW Normative Minerals (Percent)				
Q	0.000	3.483	8.828	7.283	2.126	18.179	0.000	6.852
C	0.000	0.000	0.000	0.000	0.000	0.681	0.000	0.000
OR	1.415	1.556	9.579	2.972	8.282	33.293	2.958	0.839
AB	34.974	22.698	37.830	29.152	28.990	24.897	27.170	14.955
AN	22.956	27.051	22.334	24.001	30.767	11.661	24.727	37.054
LC	0.000	0.000	0.000	0.000	0.000	0.000	0.000	0.000
NE	0.000	0.000	0.000	0.000	0.000	0.000	2.516	0.000
DI	17.560	16.351	0.401	9.908	5.992	0.000	28.429	3.022
WO	0.000	0.000	0.000	0.000	0.000	0.000	0.000	0.000
HY	18.399	24.260	16.646	19.835	19.891	8.693	0.000	33.357
OL	0.362	0.000	0.000	0.000	0.000	0.000	9.722	0.000
CS	0.000	0.000	0.000	0.000	0.000	0.000	0.000	0.000
MT	1.680	1.773	1.340	2.014	1.429	0.793	1.613	2.224
CM	0.000	0.028	0.043	0.034	0.079	0.066	0.000	0.029
IL	2.586	2.537	2.117	3.921	1.427	1.243	2.044	1.270
AP	0.074	0.271	0.904	0.901	1.042	0.507	0.843	0.410

APPENDIX B.--Abundances of major, minor, and trace elements, and normative minerals in representative rocks of the Bi'r Nifazi quadrangle--(continued).

Sample	240 385	240 386	240 387	240 388	240 389	240 392	240 393	240 395
				Major and Minor Elements (Percent)				
NA2O	0.64	2.93	2.80	0.46	1.08	1.93	2.99	1.56
MGO	3.35	8.60	4.59	12.23	12.24	6.25	5.64	10.53
AL2O3	14.78	8.94	17.54	9.57	10.07	14.05	15.93	10.46
SIO2	57.48	63.28	49.90	52.34	49.81	48.73	52.36	54.35
K2O	0.34	0.13	0.58	0.18	0.94	0.86	0.33	0.31
CAO	11.71	8.49	9.86	12.03	14.12	16.76	8.98	12.25
TIO2	0.42	0.15	0.51	0.18	0.53	0.68	1.03	0.30
CR2O3	0.00	0.18	0.02	0.12	0.06	0.00	0.02	0.08
MNO	0.16	0.11	0.17	0.17	0.13	0.13	0.18	0.09
FEO	9.74	6.57	12.92	11.29	10.01	9.06	11.26	9.07
P2O5	0.14	0.16	0.14	0.02	0.02	0.14	0.21	0.03
SUM	98.76	99.54	99.04	98.59	99.02	98.59	98.92	99.04
MG#	0.425	0.737	0.433	0.695	0.728	0.607	0.533	0.715
				Trace Elements (Parts per Million)				
CU	124	31	177	96	155	271	116	83
ZN	116	34	123	50	64	81	87	74
RB	12	12	18	10	30	32	17	13
SR	158	84	218	448	950	499	310	287
Y	14	8	9	7	18	14	26	12
ZR	52	35	50	47	78	56	77	36
NB	6	5	5	4	10	8	---	4
LA	---	3	---	10	---	16	13	---
ND	5	---	25	12	44	---	21	20
BA	126	73	131	12	71	327	73	97
CE	9	10	12	13	25	30	23	6
				CIPW Normative Minerals (Percent)				
Q	20.723	17.173	0.000	4.882	0.000	0.000	2.381	4.611
C	0.000	0.000	0.000	0.000	0.000	0.000	0.000	0.000
OR	2.054	0.797	3.478	1.058	5.593	5.139	1.967	1.862
AB	5.488	24.903	23.899	3.963	9.214	9.877	25.503	13.355
AN	36.837	10.875	33.849	23.820	20.028	27.484	29.365	20.779
LC	0.000	0.000	0.000	0.000	0.000	0.000	0.000	0.000
NE	0.000	0.000	0.000	0.000	0.000	3.628	0.000	0.000
DI	17.693	24.536	12.275	29.666	40.878	45.939	11.830	32.676
WO	0.000	0.000	0.000	0.000	0.000	0.000	0.000	0.000
HY	14.477	19.734	17.109	34.195	9.605	0.000	24.624	24.469
OL	0.000	0.000	5.974	0.000	11.894	4.815	0.000	0.000
CS	0.000	0.000	0.000	0.000	0.000	0.000	0.000	0.000
MT	1.587	1.063	2.099	1.842	1.628	1.479	1.832	1.474
CM	0.000	0.267	0.024	0.184	0.091	0.000	0.035	0.120
IL	0.806	0.284	0.979	0.346	1.023	1.309	1.972	0.579
AP	0.345	0.377	0.324	0.049	0.049	0.340	0.504	0.077

APPENDIX B.--Abundances of major, minor, and trace elements, and normative minerals in representative rocks of the Bi'r Nifazi quadrangle--(continued).

Sample	240 396	240 397	240 398	240 399	240 400	240 401	240 402	240 403
				Major and Minor Elements (Percent)				
NA2O	2.45	3.15	1.57	3.73	2.16	0.76	2.93	1.94
MGO	8.89	7.70	2.68	1.15	1.27	5.66	5.06	9.13
AL2O3	13.17	13.60	15.65	15.39	13.93	15.53	15.64	14.80
SIO2	53.34	53.15	60.41	65.23	65.89	51.76	52.33	49.75
K2O	0.45	0.22	1.98	2.90	0.58	0.33	0.19	0.47
CAO	9.63	9.58	6.71	2.71	6.95	10.78	8.31	11.35
TIO2	0.35	0.29	0.43	0.54	0.35	0.51	0.86	0.74
CR2O3	0.02	0.03	0.02	0.00	0.05	0.02	0.02	0.07
MNO	0.15	0.21	0.22	0.17	0.05	0.22	0.17	0.19
FEO	9.99	10.63	8.27	6.50	6.94	12.49	11.76	9.92
P2O5	0.03	0.13	0.39	0.37	0.25	0.13	0.31	0.13
SUM	98.47	98.70	98.32	98.70	98.41	98.18	97.58	98.49
MG#	0.656	0.605	0.411	0.282	0.287	0.493	0.490	0.672
				Trace Elements (Parts per Million)				
CU	96	45	19	135	61	126	168	139
ZN	102	106	128	128	110	132	116	79
RB	22	15	49	44	16	16	13	17
SR	189	224	445	279	422	249	102	260
Y	12	16	22	27	19	10	25	16
ZR	44	49	76	102	69	39	83	71
NB	5	5	8	9	7	---	9	6
LA	2	6	20	32	8	8	16	2
ND	18	10	9	20	19	---	---	29
BA	250	44	845	808	274	45	133	290
CE	10	15	26	43	14	2	14	9
				CIPW Normative Minerals (Percent)				
Q	1.803	0.077	21.227	21.856	32.170	9.564	4.562	0.000
C	0.000	0.000	0.000	2.093	0.000	0.000	0.000	0.000
OR	2.689	1.332	11.862	17.351	3.470	1.983	1.160	2.807
AB	21.059	26.977	13.489	31.970	18.574	6.535	25.346	16.647
AN	23.924	22.588	30.317	11.162	26.994	38.653	29.651	30.725
LC	0.000	0.000	0.000	0.000	0.000	0.000	0.000	0.000
NE	0.000	0.000	0.000	0.000	0.000	0.000	0.000	0.000
DI	19.933	20.307	0.806	0.000	5.445	12.419	8.729	20.793
WO	0.000	0.000	0.000	0.000	0.000	0.000	0.000	0.000
HY	28.195	26.095	19.190	12.592	10.875	27.497	26.177	19.914
OL	0.000	0.000	0.000	0.000	0.000	0.000	0.000	5.650
CS	0.000	0.000	0.000	0.000	0.000	0.000	0.000	0.000
MT	1.632	1.734	1.354	1.061	1.135	2.046	1.940	1.621
CM	0.030	0.039	0.024	0.000	0.070	0.026	0.028	0.100
IL	0.675	0.553	0.826	1.046	0.674	0.976	1.666	1.433
AP	0.064	0.308	0.929	0.892	0.607	0.311	0.758	0.321

APPENDIX B.--Abundances of major, minor, and trace elements, and normative minerals in representative rocks of the Bi'r Nifazi quadrangle--(continued).

Sample	240 404	240 405
		Major and Minor Elements (Percent)
NA2O	0.83	3.28
MGO	4.73	6.28
AL2O3	15.61	15.86
SIO2	56.78	51.82
K2O	0.32	0.31
CAO	10.70	10.26
TIO2	0.54	0.83
CR2O3	0.02	0.06
MNO	0.04	0.13
FEO	9.04	10.20
P2O5	0.09	0.06
SUM	98.69	99.08
MG#	0.538	0.582
		Trace Elements (Parts per Million)
CU	68	110
ZN	72	81
RB	20	11
SR	77	257
Y	18	22
ZR	55	76
NB	---	4
LA	17	1
ND	22	23
BA	46	123
CE	15	5
		CIPW Normative Minerals (Percent)
Q	18.318	0.000
C	0.000	0.000
OR	1.889	1.833
AB	7.126	28.012
AN	38.389	27.858
LC	0.000	0.000
NE	0.000	0.000
DI	12.258	19.044
WO	0.000	0.000
HY	19.282	15.828
OL	0.000	3.971
CS	0.000	0.000
MT	1.474	1.657
CM	0.028	0.082
IL	1.030	1.581
AP	0.211	0.138